Environmental and Sustainability Indicators 24 (2024) 100492

Contents lists available at ScienceDirect

Environmental and Sustainability Indicators

journal homepage: www.sciencedirect.com/journal/environmental-and-sustainability-indicators

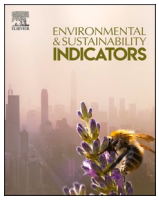

An optical satellite-based analysis of phenology and post-fire vegetation recovery in UK upland moorlands

Pia Labenski [a,b,d,*], Gail Millin-Chalabi [b], Ana María Pacheco-Pascagaza [b,e], Johannes Antenor Senn [a], Fabian Ewald Fassnacht [c], Gareth D. Clay [b]

[a] Institute of Geography and Geoecology, Karlsruhe Institute of Technology (KIT), Kaiserstr. 12, 76131 Karlsruhe, Germany
[b] Department of Geography, University of Manchester, Oxford Road, Manchester, M13 9PL, United Kingdom
[c] Department of Remote Sensing and Geoinformation, Institute of Geographic Sciences, Freie Universität Berlin, Malteserstr. 74-100, 12249, Berlin, Germany
[d] Institute of Meteorology and Climate Research - Atmospheric Environmental Research, Karlsruhe Institute of Technology (KIT), Kreuzeckbahnstraße 19, 82467 Garmisch-Partenkirchen, Germany
[e] Satellite Applications Catapult, Electron Building, Fermi Avenue, Harwell Campus, Didcot, Oxfordshire, OX11 0QR, United Kingdom

ARTICLE INFO

Keywords:
Fuel dynamics
Sentinel-2
Wildfires
Calluna vulgaris
Flammability
Harmonic modelling

ABSTRACT

Vegetation fuel dynamics in the UK's upland moorlands are important in determining landscape susceptibility to wildfire. Changes in fuel availability are influenced by phenology, land management activities or disturbances such as wildfires. Monitoring such changes is therefore essential to assess wildfire risks and impacts. This study used vegetation indices (VIs) derived from Sentinel-2 time series (2017–2023) and harmonic modelling to capture the phenology of key fuel properties and monitor post-fire vegetation recovery in four upland land cover types (acid grassland, heather, heather grassland, bog). We identified periods of high flammability, assessed the impact of wildfires on the spectral signal, and determined the time for spectral recovery as well as potential drivers of recovery times. Results showed the period of highest flammability from mid-February to early May in acid grassland, extending to early June in heather and heather grassland, and late June in bog. Summer fires caused more pronounced changes in fuel properties than spring fires, particularly in moisture-related VIs. Graminoid-dominated areas recovered rapidly (under a year), matching field observations, while dwarf shrub-dominated areas required up to three years, consistent with measurements of vegetation cover on burned areas but not with height. Spectral recovery times were primarily explained by land cover class, burn severity, season, and winter snow cover ($R2 = 0.66$). Field data highlighted pre-fire stand age's role in heather recovery and grasses' impact on spectral signals. This study improves understanding of fuel dynamics in upland moorlands through satellite monitoring, providing critical insights for more effective wildfire risk assessments and management strategies.

1. Introduction

The UK upland moorlands are unique landscapes of significant importance, containing Sites of Special Scientific Interest (SSSI) (Galbraith and Stroud, 2022), and fulfil diverse ecosystem functions. They provide a habitat for wildlife, including rare and endangered species (Van der Wal et al., 2011), sequester significant amounts of carbon (Billett et al., 2010), and are a source of drinking water for a large proportion of the UK population (Xu et al., 2018). Moreover, they provide grazing for livestock and a place for recreational activities, adding cultural and economic value (Van der Wal et al., 2011). These semi-natural ecosystems are traditionally maintained by grazing and burning, particularly rotational burning of common heather (*Calluna vulgaris* (L.) Hull, hereafter *Calluna*) for red grouse (Kirkpatrick, 2013).

However, past land-use practices such as intensive agricultural drainage, peat cutting, industrial pollution, and climate change have degraded the moorlands (Shepherd et al., 2013). Increased managed burning practices have also raised concerns about negative ecological impacts in designated conservation areas (Yallop et al., 2006). Additionally, wildfires pose a significant threat, especially during periods of dry weather and high winds (Albertson et al., 2009). Severe wildfires can damage ecosystems and release large amounts of carbon,

* Corresponding author. Institute of Geography and Geoecology, Karlsruhe Institute of Technology (KIT), Kaiserstr. 12, 76131 Karlsruhe, Germany.
E-mail address: pia.labenski@kit.edu (P. Labenski).

https://doi.org/10.1016/j.indic.2024.100492
Received 26 June 2024; Received in revised form 25 September 2024; Accepted 27 September 2024
Available online 28 September 2024

particularly when burning into the peat soil (Maltby et al., 1990). Fighting wildfires, especially in remote areas, is difficult and costly, with resource allocation becoming critical during episodes with multiple ignitions (McMorrow, 2011). The frequency of weather conditions favouring high wildfire activity is projected to double with 2 °C of global warming, exacerbating the risk of larger uncontrolled fires (Arnell et al., 2021; Perry et al., 2022). Between 2009 and 2021, 2495 wildfires were recorded in the English uplands, predominantly in mountainous, heath, bog and semi-natural grassland areas, burning the largest area of all wildfires in England (43,000 ha, 54.1%) (Forestry Commission, 2023).

Wildfires in the British uplands primarily occur in spring or summer, when plant material is flammable due to winter desiccation or low moisture during hot and dry summer periods (Albertson et al., 2010). The amount of fuel available for combustion depends on plant species and accumulation of live and dead biomass through growth and mortality (Prichard et al., 2023). Fuel dynamics in upland plant communities are naturally driven by the life cycle of *Calluna*, with its four phases pioneer, building, mature, and degeneration (Gimingham, 1972) affecting fuel characteristics such as abundance of live and dead fuels, and fine and coarser woody fuels in the *Calluna* canopy (Davies et al., 2009; Taylor et al., 2022). Fuel dynamics are further influenced by *Calluna*'s annual phenological cycle, comprising spring growth, a flowering phase lasting through August and September, and leaf senescence over late summer and autumn, increasing the relative proportion of dead material in the *Calluna* canopy over winter and early spring (Lewis et al., 2024; Mac Arthur and Malthus, 2012). Other deciduous species present in *Calluna*-dominated habitats, such as purple moor-grass *Molinia caerulea* (L.) Moench (hereafter *Molinia*), and fern *Pteridium aquilinum* (L.) Kuhn (hereafter bracken), add to a strong seasonal variation in fuel quantity and condition (Taylor et al., 2022).

Whether plant material is in a flammable state depends primarily on its fuel moisture content (FMC). The FMC of dead plant material is strongly driven by atmospheric conditions, while live vegetation FMC is also linked to plant physiology and soil moisture (Keane, 2015). Seasonal transitions from living to cured foliage cause FMC to vary, from 30% in the cured state to 250% during green-up (Burgan, 1979), with ignition likely at low FMC levels (e.g. <65% in *Molinia,* Taylor et al., 2022). In *Calluna,* live FMC can be particularly low in early spring (<45%), increasing ignition risk (Davies, 2005), while diurnal fluctuations in dead FMC can reach critically low levels over the summer (Lewis et al., 2024)

As fuel quantity and condition of the pre-fire vegetation are important drivers of fire behaviour, they directly influence the impact of the fire on the landscape. High fuel biomass in very dry condition leads to intense fires, causing severe ecosystem damage (Costa et al., 2020). Assessing the short-term and long-term effects of wildfires helps decide if and where costly restoration activities are needed. Also, understanding post-fire vegetation recovery is important for planning how long an area will be unavailable for livestock grazing and when land management actions may be required again (Kirkpatrick, 2013).

Previous studies have shown that vegetation recovery after burning in heather moorlands depends on various factors, including fire severity (Davies et al., 2010b; Grau-Andrés et al., 2019): Low-severity fires can facilitate rapid resprouting of *Calluna* shoots from stem bases, but this ability declines as plants age. High-severity fires can damage stem bases, in which case regeneration depends on seed germination (Legg et al., 1992). However, prolonged exposure of the ground to elevated temperatures destroys seed banks, resulting in slow and incomplete recovery (Maltby et al., 1990). Smouldering deep-seated wildfires in moorlands extend the vegetation recovery period and may require land intervention methods such as reseeding and plug-planting to bring the ecosystem back to pre-wildfire conditions (Rein and Huang, 2021). Without intervention, burned areas may be particularly vulnerable to invasion by other graminoids, bryophytes and herbs (Grau-Andrés et al., 2019; Velle and Vandvik, 2014). For instance, perennial *Molinia* grass, with its large and deep root system, can withstand intense fires and produces a large amount of seeds. Growth and seed production have been shown to increase after fire, resulting in high biomass production and litter accumulation (Brys et al., 2005).

While on-the-ground assessments are indispensable to understand how wildfire alters the landscape, satellite remote sensing provides a cost- and time-effective way to obtain information on pre-fire vegetation status and post-fire recovery, especially in areas with limited accessibility. Time series of vegetation indices (VIs) derived from optical sensors, e.g., Landsat, MODIS, AVHRR and Sentinel-2, have been successfully used to observe vegetation dynamics in response to wildfires or managed burns in shrub- and grassland ecosystems (Lees et al., 2021; Liu et al., 2023; Potter, 2018; Sankey et al., 2013; Villarreal et al., 2016). To monitor post-fire greening trends while accounting for seasonal variation, commonly applied methods rely on harmonic decomposition of the VI time series, e.g. implemented in BFAST (Breaks For Additive Seasonal and Trend) (Verbesselt et al., 2010) or CCDC (Continuous Change Detection and Classification) (Zhu and Woodcock, 2014). Alternatively, temporal segmentation algorithms such as LandTrendr (Kennedy et al., 2010) have been used to isolate long-term trends such as recovery by breaking time series into linear segments; however, without explicitly characterising seasonal variability (Pasquarella et al., 2022). Others have accounted for phenological variation by smoothing VI time series from undisturbed areas with moving windows to obtain an average seasonal cycle, and subtracting this cycle from time series of disturbed areas to assess recovery through the analysis of the residual time series(e.g. Lees et al., 2021).

The aforementioned studies have largely focused on Normalised Difference Vegetation Index (NDVI) to track the reemergence of vegetation greenness and phenological variation. However, NDVI is sensitive to soil background in sparse vegetation and suffers from saturation problems in dense vegetation, limiting its effectiveness in monitoring vegetation status (Wang et al., 2022). Accounting for the influence of soil background by using the Soil-Adjusted Vegetation Index (SAVI) has proven to be more effective in discriminating burn areas in heathland environments (Schepers et al., 2014). However, greenness is not the only important variable in characterising vegetation, especially from a wildfire perspective, where plant senescence and moisture status are crucial factors. Limited research has been conducted on the potential of satellite data to characterise phenology and post-wildfire vegetation recovery in moorland habitats.

Considering fuel moisture, Al-Moustafa et al. (2012) showed that vegetation indices combining near-infrared (NIR) and shortwave infrared (SWIR) reflectance derived from airborne hyperspectral imagery strongly correlate with live FMC in *Calluna* plots at a moorland site. Similarly, Badi (2019) found a strong positive relationship between the Normalised Difference Water Index (NDWI) (Gao, 1996), also referred to as Normalised Difference Moisture Index (NDMI) (Wilson and Sader, 2002), calculated for multi-temporal Sentinel-2 and Landsat imagery and measured *Calluna* FMC.

Senescent biomass is less frequently assessed in remote sensing studies, including those in upland moorland vegetation. However, Metzger et al. (2017) found that estimates of biomass and the green ratio in a temperate grassland fen based on NDVI were poor due to the presence of standing senescent biomass. Guerini Filho et al. (2020) estimated senescent plant biomass in the grasslands of the Brazilian Pampa from Sentinel-2 data, using among others the Plant Senescence Reflectance Index (PSRI), with moderately accurate results. PSRI calculated from field spectroscopy has been shown to indicate phenological change in upland vegetation species and was useful for discriminating between plant functional types (Cole et al., 2014). However, PSRI based on spectroradiometer measurements had limited correlation with leaf pigment content of *Calluna* (Nichol and Grace, 2010), so the applicability of the index for monitoring plant senescence across moorland land cover classes using satellite data remains to be investigated.

Lees et al. (2021) assessed vegetation regeneration in UK moorlands

after low-severity management fires using NDVI time series, but suggested a comparison with other indices and field assessments of vegetation recovery would be beneficial. Millin-Chalabi (2016) used pre- and post-fire Synthetic Aperture Radar (SAR) signals to characterise wildfire burn scars and assess their persistence in peat moorlands. The study showed that increased SAR backscatter of burned areas can persist for more than six months post-fire and indicate incomplete vegetation recovery. However, the pre- and post-burn conditions and the effect of wildfires of varying severity on the optical remote sensing signal of different upland land cover classes have not been investigated. This is due to the challenges posed by frequent cloud cover in upland environments particularly in the UK (Armitage et al., 2013).

Therefore, in this study, we applied a multi-index approach based on time series of Sentinel-2 data and harmonic modelling to capture key fuel characteristics of UK upland vegetation and provide a more comprehensive understanding of both phenology-driven fuel dynamics and vegetation recovery after wildfire. We utilised optical VIs, which have proven useful in previous studies, to highlight specific vegetation properties. We focused on SAVI as a proxy for live/green vegetation cover, PSRI for dead/senescent vegetation cover, and NDMI as proxy for FMC. Additionally, we included the commonly used indices NDVI and Normalised Burn Ratio (NBR) in our analysis. The NBR has become a standard index to assess burn severity across different ecosystems (e.g. Boelman et al., 2011; Schepers et al., 2014). Our study aimed to evaluate the potential of optical remote sensing to characterise fuel dynamics in upland land cover classes and enhance our understanding of wildfire impacts on the landscape by addressing the following research questions.

- What is the remotely sensed phenology of key fuel properties of UK upland land cover classes, and how is it related to records of wildfire occurrence?
- To what extent do remotely sensed fuel properties change, and what is the timeframe for their recovery following a wildfire?
- How do remote sensing observations align with field measurements of vegetation recovery?
- How are remotely sensed vegetation recovery times influenced by environmental factors?

2. Methods

2.1. Study area

This study focuses on the moorlands of the South Pennines in northern England, encompassing the Peak District National Park (PDNP) and Marsden Moor. The PDNP covers an area of 1438 km^2, ranging in altitude from 12 to 636 m. While the northern part and the eastern and western margins are characterised by moorland and gritstone formations of the Dark Peak, limestone plateaus and gorges dominate the White Peak in the central and southern parts (PDNPA, 2013). The land cover classes of the Dark Peak are mainly heather moorland, bog, and acid grassland, whereas the White Peak is characterised by calcareous and improved grassland, and woodland (Fig. 1). Wildfires recorded in the PDNP over the past decades have been concentrated in the Dark Peak (Moors for the Future, 2023). Therefore, acid grassland, heather, heather grassland, and bog are the focus of this study. The UK Centre for Ecology and Hydrology (UKCEH) Land Cover Map (LCM2021) (Marston et al., 2022) defines these land cover classes as follows: 'acid grassland' can have a variable composition of grasses, rushes, herbs, and sedges, but is often dominated by *Molinia*. 'Heather' land cover is distinguished from 'heather grassland' by a cover of more than 25% *Calluna*. 'Bog' includes areas of ericaceous, herbaceous, and moss species on deep peat soils (>0.5 m).

2.2. Workflow

The flowchart in Fig. 2 gives an overview of the datasets used and analyses carried out in this study, which are described in detail in the following sections.

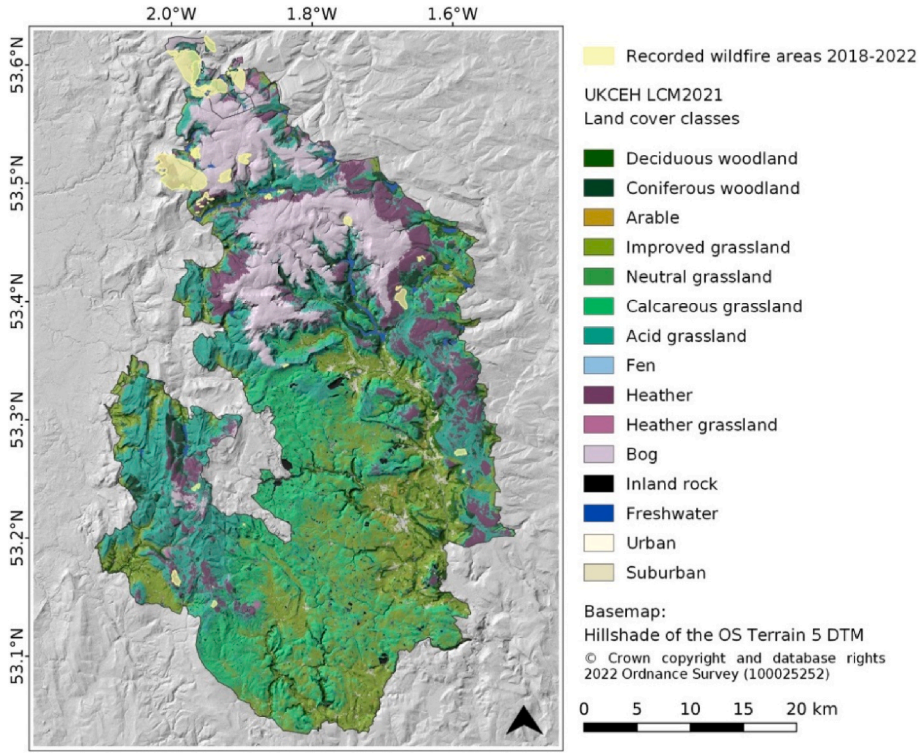

Fig. 1. South Pennines study area showing the land cover classes and wildfire areas considered in this study.

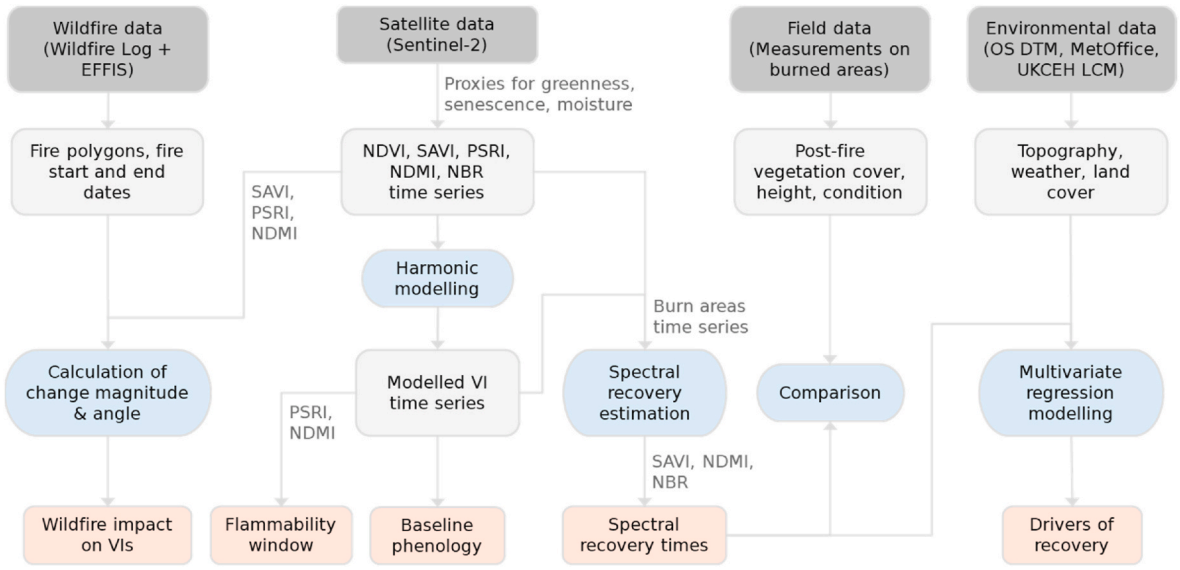

Fig. 2. Overview of the workflow of this study.

2.3. Datasets

2.3.1. Satellite data

We obtained time series of Sentinel-2 surface reflectance (harmonised Level-2A collection) with a spatial resolution of 10 m from Google Earth Engine (GEE). All scenes from 2017 to 04-01 to 2023-09-20 that covered the study area and had a maximum cloud cover of 50% were included. Clouds were masked based on the Sentinel-2 cloud probability product using a threshold of 40% probability for masking. Cloud shadows were removed based on NIR reflectance, while snow and ice were masked based on the scene classification band (SCL) of the Sentinel-2 product. For each of the masked scenes, we calculated the VIs listed in Table 1 using the eemont package (Montero, 2021). All processing was done via the GEE Python API in Google Colab.

2.3.2. Wildfire data

Records of wildfire incidents in the South Pennines were downloaded from the local wildfire recording system managed by the Moors for the Future Partnership (Moors for the Future, 2023). The database contains polygons that delineate wildfire perimeters based on field observations of burned areas, as well as additional information such as fire start and end dates. We cross-checked the polygons from the wildfire log with wildfires recorded in the European Forest Fire Information System (EFFIS) (San-Miguel-Ayanz et al., 2012) to ensure no large wildfires were missed. We obtained 45 wildfire polygons covering a five-year period from 2018-01-01 to 2022-12-31. For each fire, we visually inspected the closest cloud-free pre- and post-fire RGB and NBR images from Sentinel-2. We used the post-fire imagery to slightly correct the position and shape of some wildfire polygons, which were likely affected by positional inaccuracies of the GPS devices used for field recording. As a measure of fire severity, we calculated the differenced NBR (dNBR) for each wildfire area by subtracting post-fire from pre-fire NBR of the previously selected images. We removed wildfires with a dNBR<0.1 from the dataset, as we expected a very weak signal in the remote sensing indices from these low-severity fires. We also removed fires that were obviously management burns, as indicated by the many small burn strips in the satellite imagery. Ultimately, we obtained a dataset of 38 wildfire polygons with different severities and burned areas in the four land cover classes (Fig. 3).

Table 1
Sentinel-2 VIs used in this study. Bands were renamed as follows: B8:NIR, B9: NIR2, B11: SWIR1, B12:SWIR2, B6:RedEdge2.

Index	Proxy for	Equation	Reference
NDVI	Vegetation greenness, live biomass	$\frac{NIR - Red}{NIR + Red}$	Rouse et al. (1974)
SAVI	Vegetation greenness, live biomass, accounts for soil effects	$\frac{NIR - Red}{NIR + Red + L}(1 + L)$, $L = 0.5$	Huete (1988)
NDMI	FMC	$\frac{NIR - SWIR1}{NIR + SWIR1}$	Wilson and Sader (2002)
PSRI	Vegetation senescence, dead biomass	$\frac{Red - Blue}{RedEdge2}$	Merzlyak et al. (1999)
NBR	Vegetation structure, intact vegetation biomass	$\frac{NIR2 - SWIR2}{NIR2 + SWIR2}$	Coffelt and Livingston (2002)

2.3.3. Field data

We collected data on post-fire vegetation recovery in 14 wildfire areas in the South Pennines during a field campaign 3–14 July 2023. Long-term vegetation recovery is ideally assessed over several years, but adopting a space-for-time approach is a common strategy in ecology (e.g. Harper, 2020; Thomaz et al., 2012). We also used this approach, acknowledging that the results must be interpreted cautiously, as the burn conditions of the individual wildfires were different. We visited two to three wildfire areas from each year between 2018 and 2023 and measured vegetation cover and height in two to six plots per area, and in 15 plots in the large Tameside wildfire area (also commonly known as the Saddleworth Moor fire, e.g. Graham et al. (2020)) (Table S1, supplementary material). The locations of the 10 × 10 m plots were selected to encompass landscape heterogeneity. We used an adapted version of the FIREMON point intercept method (Lutes et al., 2006) to sample vegetation cover, condition, and height. The sampling was conducted along three parallel 10 m transects positioned at 0, 5, and 10 m along the plot baseline. At 50 cm intervals, we documented the presence of the following plant species or functional groups: grass, rush, moss, heather, bell heather, bilberry, crowberry, bracken. We noted the condition of the plants, categorising them as live, dead/senescent or charred. Additionally, we measured vegetation height at 2 m intervals. This data was used to calculate average cover per plant type and condition, as well as average vegetation height at different times post-fire. Due to limited resources and landscape heterogeneity, we did not establish control plots in unburnt areas. The collected information on post-fire vegetation

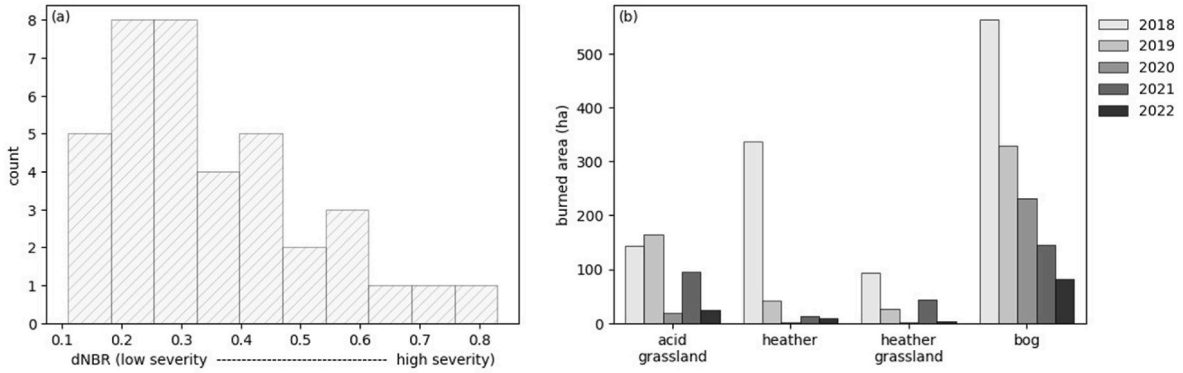

Fig. 3. (a) Burn severity of individual wildfires and (b) burned area in different land cover classes per year.

condition, cover, and height on burned areas was used for comparison with remote sensing estimates of vegetation recovery. However, a direct validation of the recovery estimates per wildfire area was not possible because the field data only covered one point in time per area, and the vegetation composition of individual wildfire areas varied considerably even within the same classified land cover. In addition to assessing long-term vegetation recovery, we captured the immediate post-fire response at one site (Standedge) burned on May 3, 2023 by visiting the area repeatedly on May 4, June 7, and July 3, 2023. We collected vegetation data on three fixed plots inside the wildfire area and two plots outside the area. Measurements were carried out as described earlier, except that the sampling interval was 1 m along each transect.

2.4. Phenology analysis

2.4.1. Estimation of baseline phenology for the South Pennines

To establish a baseline phenology of vegetation fuel properties as captured by remotely sensed VIs, we randomly sampled 500 satellite image pixels per land cover class across the South Pennines. These samples were collected from every available Sentinel-2 scene, excluding known wildfire areas. Due to frequent cloud cover in the study area, the number of valid pixels per scene varied significantly. Therefore, we chose to keep only 30 pixels per land cover class and discard time steps with less than 30 valid pixels. We computed the bivariate kernel density of the 30 pixel values per time step using a Gaussian kernel density estimation following the 'npphen' approach (Chávez et al., 2023) to display the frequency distribution of the VI values along the time series. Next, we calculated the mean over the 30 pixels per time step to obtain the average time series for each VI and land cover class. We removed any remaining outliers in the time series caused by undetected clouds/haze by applying a Hampel filter (Pearson et al., 2016). Outliers at the time series ends that could not be detected using the Hampel filter were removed using fixed thresholds for each spectral index that were determined after careful investigation of the data: NDVI<0.4, SAVI<0.1, NDMI>0.5, PSRI<−0.05, NBR>0.7. We modelled the outlier-filtered time-series of each VI using a harmonic model consisting of a series of sine and cosine terms defined in *Equation (1)* (e.g. Zhu and Woodcock, 2014):

$$y_t = \beta_0 + \beta_1 t + \beta_2 \cos(\omega t) + \beta_3 \sin(\omega t) + \beta_4 \cos(2\omega t) + \beta_5 \sin(2\omega t) + \beta_6 \cos(3\omega t) + \beta_7 \sin(3\omega t) \quad (1)$$

β_0 and β_1 are the overall mean and the inter-annual trend, respectively, β_2 to β_7 capture the intra-annual variation of the signal at different frequencies $\omega = 2\pi/365.25$. The time series model was fitted using the Levenberg-Marquardt least squares optimisation implemented in the Python package 'lmfit' (Newville et al., 2014). From the modelled time series, we extracted several phenological characteristics such as mean, amplitude, maxima, minima, day of the year of minima and maxima, as well as model performance metrics.

2.4.2. Identification of periods of high vegetation flammability

We identified periods of high vegetation flammability from the baseline phenology of individual wildfire areas. We hypothesised that a combination of low FMC and a high proportion of dead plant material, as indicated by low NDMI and high PSRI values, would result in higher probability of successful ignition. We thus identified the overlapping periods of lowest NDMI and highest PSRI values in the annual time series by extracting the intersection points of the two VIs around their global minimum (NDMI) and maximum (PSRI). We compared the identified flammability periods with the actual wildfire occurrence dates.

2.5. Wildfire effects and recovery

2.5.1. Estimation of wildfire impact on VIs

We assessed the immediate impact of wildfires on VIs obtained from Sentinel-2 by calculating the change magnitude and change angle for key indices, namely SAVI, NDMI, and PSRI. These indices serve as primary indicators of fuel properties: green biomass, fuel moisture, and senescent biomass. Calculations were performed separately for each land cover class and for the meteorological spring (MAM) and summer (JJA) seasons. We calculated change magnitude as the Euclidean distance between the pre- and post-fire spectral data points of a land cover class and season in a 3-dimensional Cartesian space whose axes correspond to SAVI, NDMI, and PSRI. Change angle was determined from the angle between the two vectors drawn from the origin to the pre- and post-fire spectral data points according to the Spectral Angle Mapper (SAM) algorithm (Kruse et al., 1993). SAM is a common measure of the similarity between two spectral vectors, with a smaller angle indicating greater similarity. Finally, we obtained a combined estimate of the impact of wildfires on VIs by normalising both change magnitude and change angle to the range [0, 1] and then averaging the two.

2.5.2. Estimation of spectral recovery times

We estimated recovery times of the different VIs after wildfire. Therefore, we extracted the average VI time series for each land cover class within a wildfire polygon. We did not filter these time series for outliers, as potential outliers could also represent the signal from the fire. The pre-fire time series was modelled using the model from Equation (1) and then extrapolated to the post-fire period. In cases where the pre-fire period had less than two years of valid acquisitions and was difficult to model, we extracted the VI time series for the same land cover class within a 1 km buffer zone of the wildfire polygon as a substitute to obtain the model parameters. We found that the highly mosaicked and managed landscape resulted in a higher spatial variability of the observed phenology within a single land cover class compared to the temporal variability due to interannual variations in climatic conditions. Consequently, we used the buffer approach only in a limited number of

cases. We subtracted the modelled and extrapolated time series from the actual time series of the wildfire area to obtain the residuals. To determine the time of spectral recovery, we repeatedly compared the distribution of the residuals in the post-fire period to the distribution of the pre-fire residuals. For this purpose, we used moving windows of four different sizes (n = 3, 5, 10, 20), each shifted by one observation from the first post-fire satellite image to the present. We continued this process until the post-fire residuals within the window were no longer significantly different from the pre-fire residuals, as tested by Welch's test ($\alpha = 0.05$). If no significant difference could be found for three consecutive time steps, the area was declared as spectrally recovered. We used different window sizes to make the approach more robust to the effects of outliers, data gaps, and different recovery rates. As a visual analysis of the residuals showed that the recovery time tended to be underestimated, we obtained the final recovery time of each VI as the maximum recovery time across the four window sizes. However, for acid grassland we used a window size of five for the final recovery time, as spectral recovery was fast and overestimated with larger windows. As a single estimate of the VI-derived recovery rate per wildfire event and land cover class, we used the maximum of SAVI, NDMI and NBR recovery. We did not include PSRI in final recovery estimation because it was the index with the weakest model fit and highest scatter, which sometimes led to unrealistic recovery estimates. Instead, we used NBR, as it is sensitive to vegetation structure and therefore expected to provide a robust estimate of the long-term vegetation recovery (e.g. Pickell et al., 2016).

2.5.3. Analysis of drivers of spectral recovery times

We investigated the effects of various environmental variables and wildfire-related factors (Table 2) on recovery times using multiple linear regression models. We extracted topographic information from the OS Terrain 5 DTM product (Ordnance Survey, 2023). We obtained meteorological data from the collection of gridded and monthly aggregated land surface observations over the UK at 1 km resolution (Hollis et al., 2023) and summarised them for different pre- and post-fire periods. Since recovery times varied across land cover classes within a wildfire area, we treated each land cover class of a burned area as an individual sample when calculating correlation coefficients and building regression models. The sample size was n = 74. We used Ordinary Least Squares (OLS) and tested different combinations of the variables most strongly correlated with recovery rate. We visually inspected the model residuals for normality and homoscedasticity. The final model to explain recovery was selected based on R^2 and the Akaike's Information Criterion (AIC).

Table 2
Variables used to explain spectral recovery times.

	Variables	Assumed influence on
Topography	Elevation	Local microclimate
	Slope-aspect interaction	Fire dynamics, fire severity, soil conditions
	Northness & eastness	Fire dynamics, fire severity
Wildfire	Fire severity (dNBR)	Regeneration capacity
	Size	Distance to seed sources
	Season	Phenological stage, weather conditions
Vegetation	Land cover class	Specific flammability, regeneration capacity
Weather	Precipitation	Soil moisture, erosion
	Temperature	Growth activity
	Wind speed	Exposure, erosion, seed dispersal
	Sunshine duration	Seed germination, growth
	Days of ground frost	Soil conditions
	Days of snow cover	Soil conditions

3. Results

3.1. Baseline phenology for the South Pennines

The phenology analysis revealed similar patterns between the land cover classes. As expected, the remotely sensed cover of green vegetation is lowest over winter and spring (Fig. 4), although NDVI and SAVI indicate a different day of year (DOY) for the location of the minimum (DOY 355-103). The lowest FMC reflected in low NDMI values is reached around the end of March/beginning of April (DOY 89–106). The latter period is also characterised by highest plant senescence (PSRI). NBR patterns closely follow NDMI as both rely on NIR and SWIR reflectance. The extracted phenological characteristics of each land cover class are listed in Table S2 (supplementary material). While the seasonal patterns are similar, acid grassland and heather grassland exhibit larger amplitudes in the variation of green and senescent biomass ($A_{SAVI/NDVI} = 0.14$, $A_{PSRI} = 0.08$) than heather and bog ($A_{SAVI/NDVI} = 0.10$, $A_{PSRI} = 0.06$). Grass-dominated land cover classes also generally have higher FMC (mean NDMI = 0.18) than heather-dominated land cover (mean NDMI = 0.12). Wildfire occurrences accumulate in spring when plant senescence is high and FMC is low in all land cover classes. This period also has the highest density of valid data points (available clear-sky observations), indicating more cloud-free days, which may be related to the dominance of high-pressure systems that can promote fuel dryness (Perry et al., 2022). Single wildfire events occurring in summer partly coincide with prolonged periods of exceptionally dry conditions, as indicated by lower-than-average NDMI observations in the summer of 2018.

3.2. Spring flammability window and pre-fire fuel conditions

In all land cover classes, the period of higher vegetation flammability starts in mid-February (Fig. 5). It ends in early May in acid grassland, and lasts until early June in heather and heather grassland. Bog has the largest flammability window, extending into mid to late June. These periods encompass 71% of the recorded wildfires in acid grassland, 73% in heather, 90% in heather grassland, and 81% in bog. The start and end days for each land cover class are provided in Table S3 (supplementary material).

When comparing the remotely sensed fuel conditions in areas affected by wildfires in spring and summer to the average phenology in the South Pennines for the respective season (Fig. 6), a notable finding emerges: particularly in spring, the areas impacted by wildfire showed remarkably low NDMI values compared to the average phenology. Furthermore, they had a significantly higher proportion of senescent (PSRI) relative to live vegetation cover (SAVI) just before the outbreak of the fire, especially in acid grassland and heather grassland. In summer, fuel conditions are generally less variable and characterised by less senescent cover than in spring. However, atypical conditions in wildfire-affected areas were only observed for one fire event in bog and heather (lower NDMI), which occurred in the summer of 2018 and represents the exceptionally large Tameside wildfire (circled cross in Fig. 6).

3.3. Wildfire impact on VIs

The immediate impact of wildfires on fuel properties, as determined from remotely sensed VIs, was more pronounced in summer compared to spring. This is evident in the greater magnitude and angle of change observed between pre- and post-fire data of SAVI, PSRI, and NDMI across all land cover classes (Fig. 7, Table 3). SAVI and NDMI showed a strong decrease after summer fires (both −0.27), indicating a substantial reduction in live green biomass, whilst there was a less pronounced decrease in spring (−0.09 and −0.13), where they had lower pre-fire levels. PSRI changed slightly, showing on average a small reduction after spring fires (−0.07) and a small increase after summer fires (+0.07). Overall, wildfire impact on VIs differed only slightly between

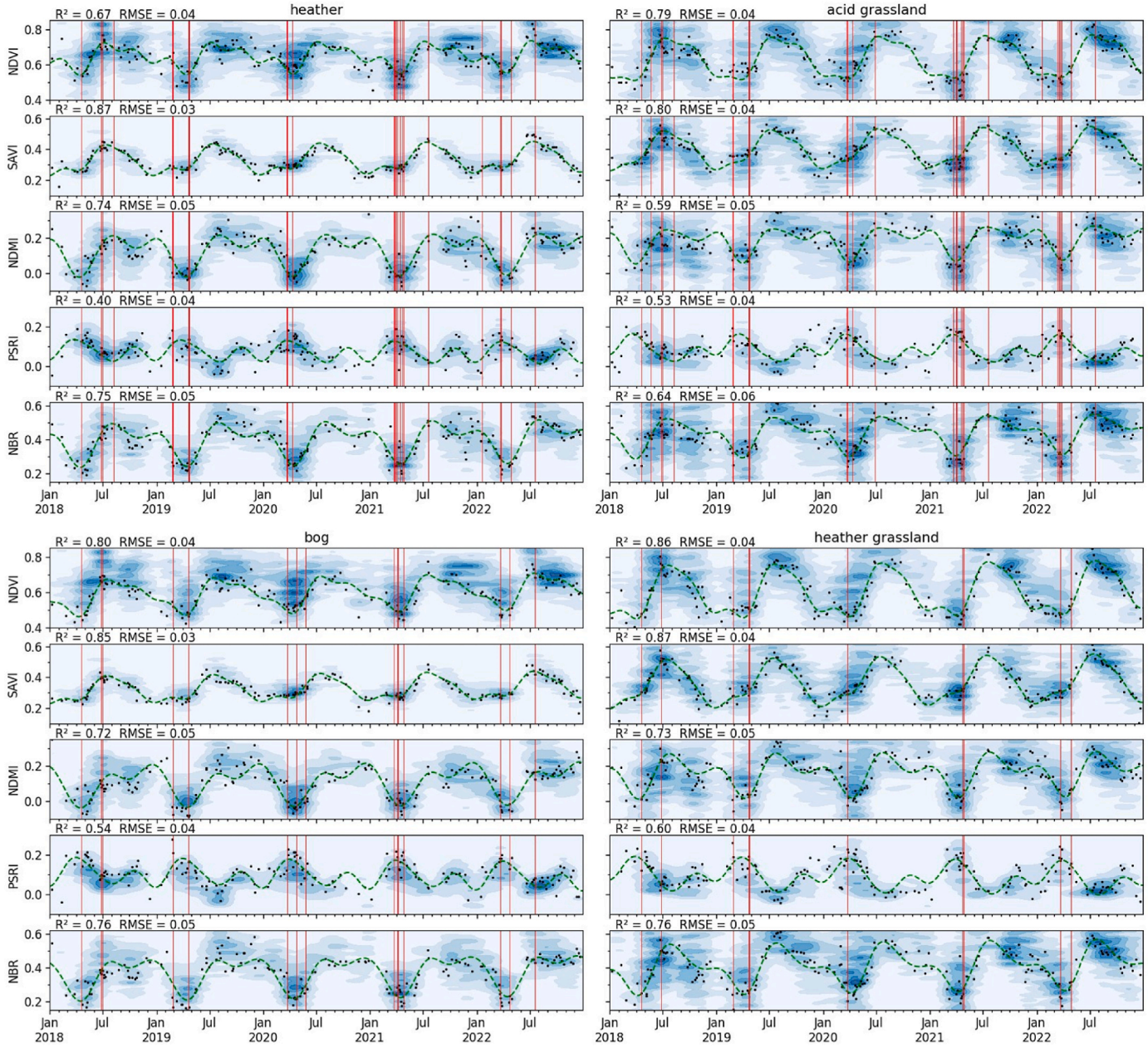

Fig. 4. Phenological patterns of the VIs in the four land cover classes. Black dots show the mean values of the VIs in the South Pennines over the five years of observation, while the green dashed lines represent the modelled time series. Vertical red lines indicate wildfire start dates. Darker shades of blue indicate a higher bivariate density of observations (in time and across sample pixels). (For interpretation of the references to colour in this figure legend, the reader is referred to the Web version of this article.)

the different land cover classes, compared to the large variability in effects between fires (Table S4, supplementary material).

3.4. Spectral recovery of VIs

The spectral recovery time varied across land cover classes. Owing to the skewed dispersion of values over the different wildfire events, we use the 75th percentile (PC75) for the comparison here. Acid grassland consistently had the shortest recovery times, with PC75 values ranging from 105 to 180 days for the different VIs. Heather grassland followed with PC75 spanning 168–372 days. In bog areas, recovery estimates were more variable: PSRI recovered the fastest with PC75 being 158 days, while NBR and NDMI had slower recovery times of 470 and 686 days, respectively. NDVI and SAVI also gave different results for the recovery of greenness in bog areas, with PC75 values of 264 and 776 days, respectively. Heather recovery times were the longest with PC75 between 584 and 801 days for all VIs except PSRI, which showed a faster recovery time of 345 days (as shown in Figs. 8 and 9). Notably, the variability in recovery times was higher in heather and bog areas compared to acid grassland and heather grassland, particularly between individual wildfire events.

Most wildfire areas in the South Pennines showed relatively minor changes ('low impact') in spectral VIs and tended to recover spectrally in less than two years (Fig. 10, quadrant I). Large spectral changes ('high impact') and rapid recovery, often within one year, were observed particularly in acid grasslands (quadrant II). In contrast, large spectral changes coupled with slower recovery, exceeding two years, were primarily observed in heather and bog (quadrant III). Similarly, smaller spectral changes and slower recovery were prevalent in these two land cover classes (quadrant IV). A significant positive correlation between

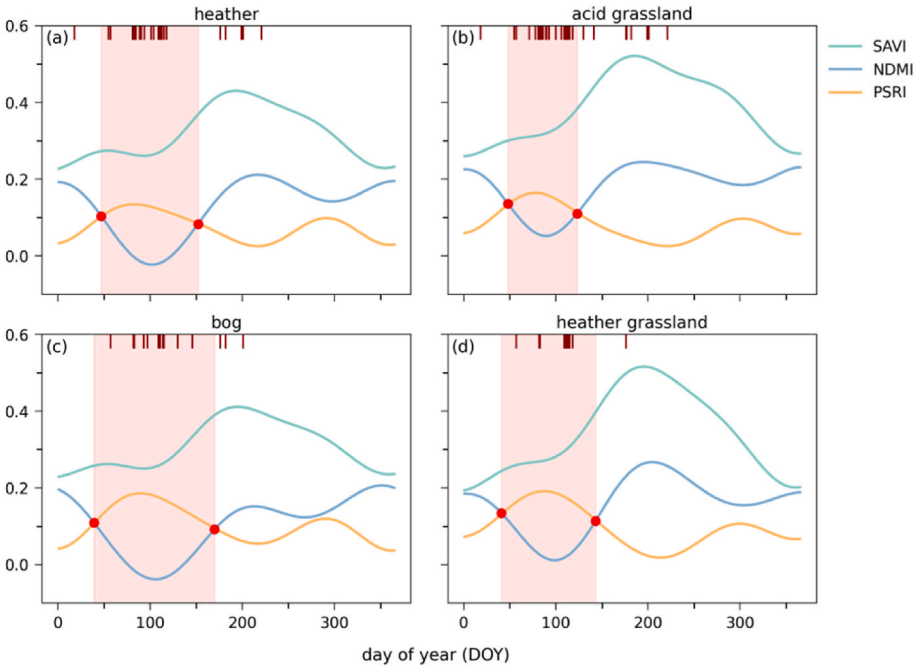

Fig. 5. Flammability window of each land cover class calculated from the average baseline phenology of VIs. Red lines at the top of each plot indicate the occurrence of wildfires. (For interpretation of the references to colour in this figure legend, the reader is referred to the Web version of this article.)

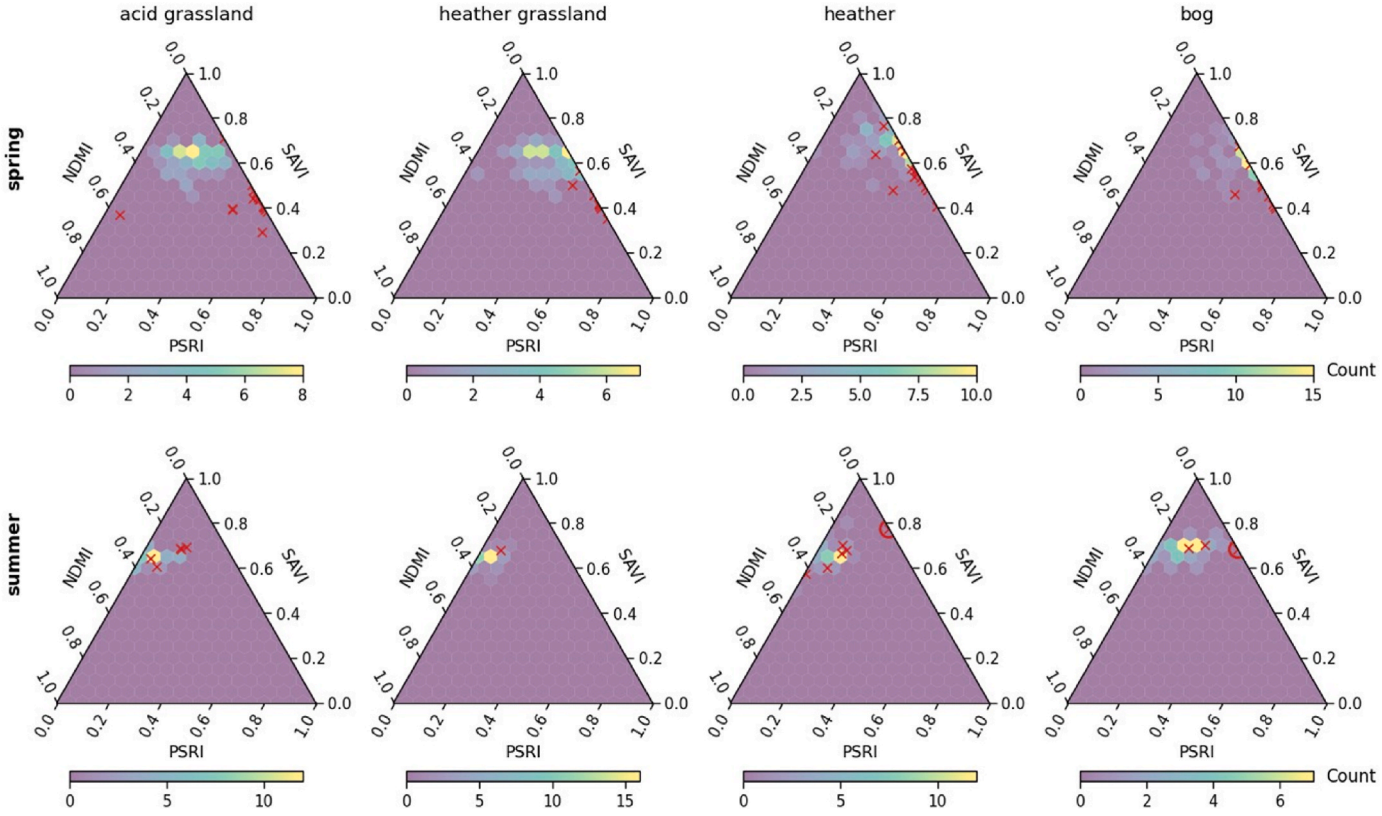

Fig. 6. Ternary plots showing the occurrence frequency of typical proportions of SAVI, PSRI, and NDMI during spring and summer in the South Pennines' land cover classes derived from their baseline phenology (coloured filling). Red crosses show the conditions shortly before a wildfire outbreak. Note that the axes do not display the actual VI values, but their proportion (all three VIs sum to 1). Circled cross represents the Tameside wildfire in 2018. (For interpretation of the references to colour in this figure legend, the reader is referred to the Web version of this article.)

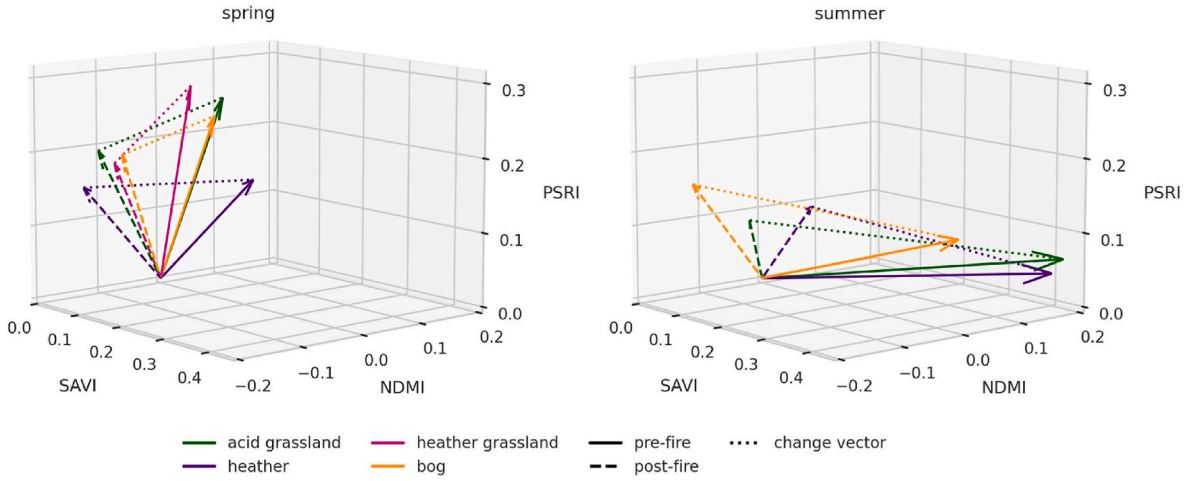

Fig. 7. Vectors representing average pre- and post-fire VIs for each land cover class separated by season. Since there was only one fire in heather grassland in summer, the vectors are not displayed here.

Table 3
Mean change magnitude and change angle between pre- and post-fire observations of SAVI, NDMI, and PSRI and their standard deviations. Values for heather grassland are not shown due to only one wildfire occurrence.

Land cover	Season	Magnitude	Angle
Acid grassland	Spring	0.27 ± 0.11	42.1° ± 22.3°
	Summer	0.47 ± 0.22	62.5° ± 32.8°
Bog	Spring	0.17 ± 0.06	25.1° ± 11.9°
	Summer	0.45 ± 0.27	65.6° ± 32.1°
Heather	Spring	0.25 ± 0.12	42.2° ± 21.3°
	Summer	0.49 ± 0.34	66.5° ± 42.6°
Heather grassland	Spring	0.22 ± 0.09	32.3° ± 17.5°

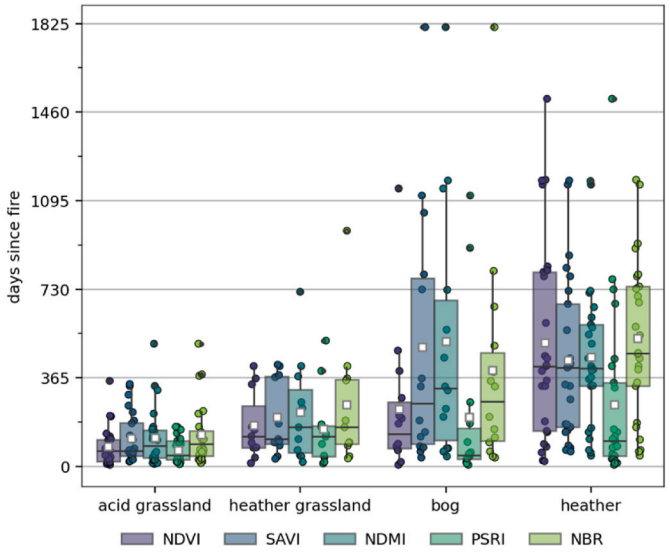

Fig. 8. Recovery times of the VIs for different land cover classes. Mean values are shown as white squares.

spectral change and recovery time was observed only for heather land cover (Spearman's r = 0.50, p-value = 0.02).

3.5. Field-measured vegetation recovery

While we describe the field data as a true chronosequence for ease of reading, it is important to emphasise that it is a pseudo-time series created from space-for-time sampling. Vegetation cover in the sampled wildfire areas averaged approximately 69% in the first year after the fire (Fig. 11a), with subsequent years showing further recovery. Vegetation heights also increased over time, but differed greatly between wildfire areas of the same year (i.e., different sites, Fig. 11b). We therefore differentiated our plots according to the dominance of either graminoids or dwarf shrubs. The graminoid-dominated plots had on average 96% vegetation cover in the first year after the fire (Fig. 11 c), which aligns with the observed VI recovery times of less than one year in grassland land cover classes (Fig. 8). In the first year following fire, we recorded the highest grass heights (Fig. 11d). While vegetation cover remained high in subsequent years, heights decreased to a lower level. In the dwarf shrub-dominated land cover classes, average vegetation cover and height were initially low in the first year after the fire (48% and 12 cm, respectively). Vegetation cover increased to about 69% in the second year and 85% by the third year post-fire, while vegetation heights remained low for the first three years and reached heights comparable to those in graminoid-dominated areas only in the fourth to fifth year after fire. The development of live vegetation cover (Fig. 11e) roughly followed the pattern of total vegetation cover, but the proportion of dead vegetation was higher in graminoid-dominated plots than in dwarf shrub-dominated plots, especially from the second year post-fire (Fig. 11f).

An assessment of vegetation recovery immediately following the Standedge wildfire shows that vegetation recovers rapidly in such grass-dominated areas (Fig. 12). Within only one month post-fire, live vegetation cover in the burned area was not significantly different from the unburned area, where spring growth had just started. The (visible) cover of charred vegetation in the burned area also decreased rapidly. The cover of senescent plant material was initially high in the unburned area, but visually decreased as new grass shoots emerged. Hence, two months after the fire, burned and unburned areas had similar measured cover of dead vegetation. Vegetation height in the burned area was comparable to the unburned area two months after the fire. Fig. S1 (supplementary material) provides photographic evidence of the burned area's recovery.

3.6. Drivers of spectral recovery

To explain spectral recovery times we selected a model that achieved an adjusted R^2 of 0.58 and used land cover class and season as categorical variables, along with the continuous variables burn severity and days with snow cover (Table 4). When each of the four variables was excluded from the model, we found that land cover class had the strongest influence (reduced adj. R^2 = 0.32), followed by burn severity

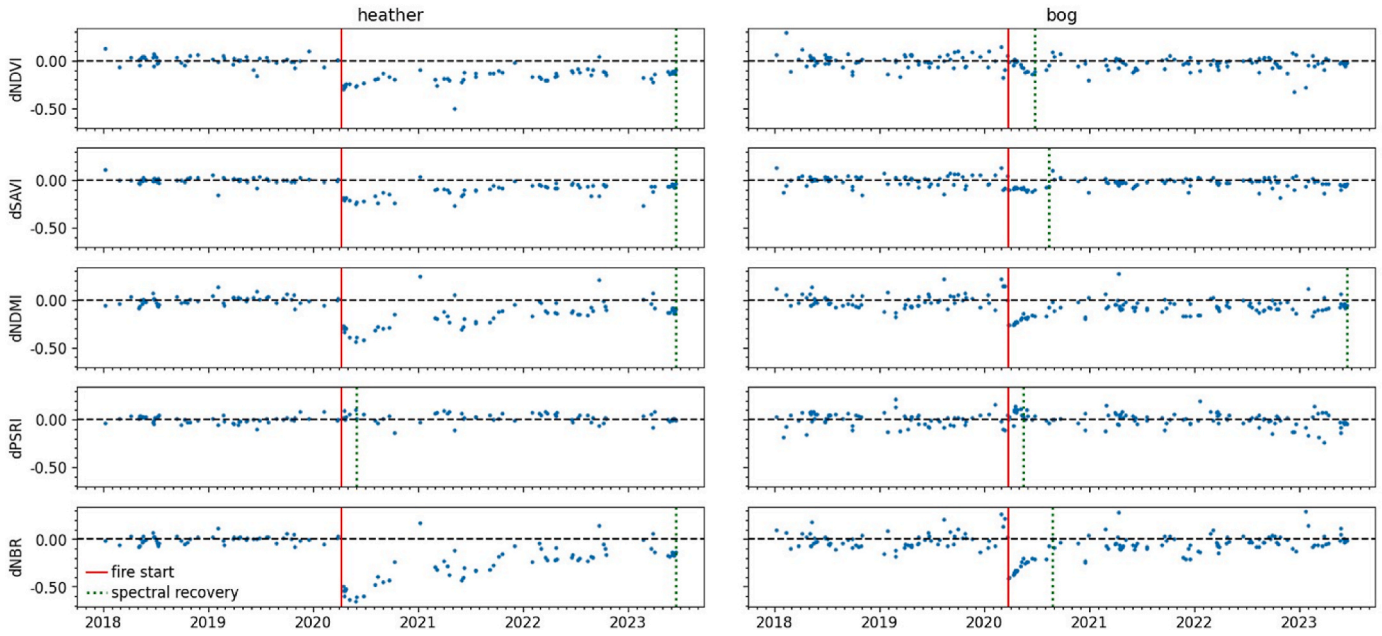

Fig. 9. Example of the different recovery trajectories of the VIs for two wildfire events in heather (West of Didsbury intake) and bog (Kirklees) that occurred in spring 2020. Red vertical line denotes fire occurrence. Dashed green vertical line denotes point of spectral recovery. (For interpretation of the references to colour in this figure legend, the reader is referred to the Web version of this article.)

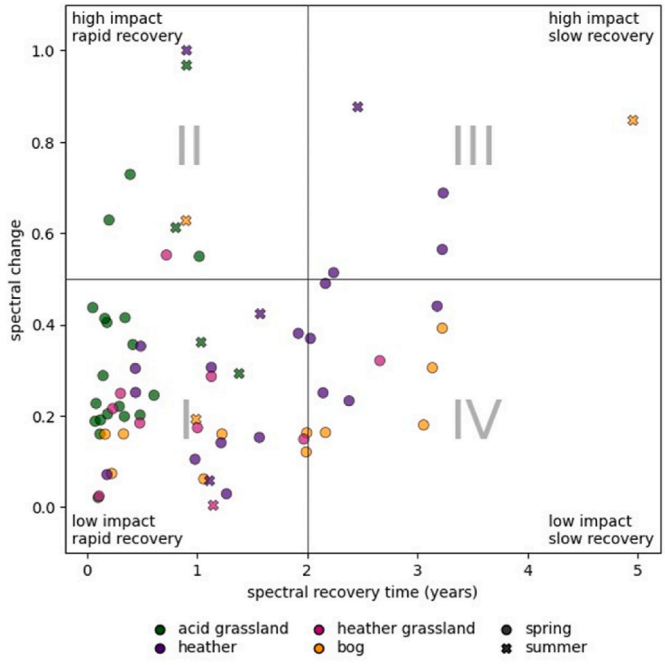

Fig. 10. Mean recovery time of the VIs for each wildfire area versus the spectral change (combined measure of change magnitude and change angle).

(0.46), days with snow cover (0.53), and season (0.56). Recovery times increased with burn severity. In comparison to the reference category acid grassland, bog and heather were estimated to have recovery times more than one year longer, while heather grassland had recovery times less than one year longer. Summer fires recovered approximately six months faster than spring fires. Recovery times were further estimated to increase with more days of snow cover in winter. When interactions between land cover class, season, and burn severity were included in the model (Table 5), the adjusted R^2 increased to 0.66. This model revealed that burn severity in acid grassland had no significant effect on recovery times, in contrast to bog and heather. Generally, the correlations between recovery time and other environmental variables were low, with significant values ($\alpha = 0.05$) for elevation (Pearson's $r = 0.35$), temperature, and sunshine duration in the year post-fire ($r = -0.30$ and -0.31), wind in the year post-fire ($r = 0.31$), and days with groundfrost in winter ($r = 0.32$). However, none of these variables were significant factors in the selected regression model.

4. Discussion

4.1. Baseline phenology and flammability window

Phenological patterns of key fuel characteristics are captured by remotely sensed VIs as they show expected fuel conditions (low moisture, high plant senescence) at times of increased wildfire activity. Modelling the time series effectively illustrates the typical annual progression with acceptable accuracy for most VIs ($R^2 = 0.59$–0.87) except PSRI ($R^2 = 0.40$–0.60). However, extended gaps in the time series resulting from frequent cloud cover, particularly in winter, introduce uncertainty to the modelled second peak in NDMI/NBR and the second trough in PSRI in January. Gaps in this section of the dataset are perhaps less problematic as this period tends to have lower wildfire activity, though it is an important period during which fuel can desiccate (Hancock, 2008). Spectral measurements by Cole et al. (2014) between April and September in the PDNP also showed clear seasonal patterns in reflectance for both dwarf shrubs and graminoids, with the largest amplitudes confirmed in graminoid species. The higher stability of the SAVI time series compared to NDVI in our study suggests that SAVI is a more reliable proxy for greenness, particularly for land cover classes with bare ground exposure. The VIs also capture specific fuel properties of the land cover classes, such as the low FMC of *Calluna* and its pronounced drop in early spring (Davies et al., 2010a), consistent with previous studies that successfully related FMC in upland vegetation to spectral indices such as NDWI or Moisture Stress Index (MSI) (Al-Moustafa et al., 2012; Badi, 2019).

NDMI and PSRI further allow the identification of periods when vegetation is in a condition that is critical for burning and could be used as a complement to meteorological fire danger indicators such as the

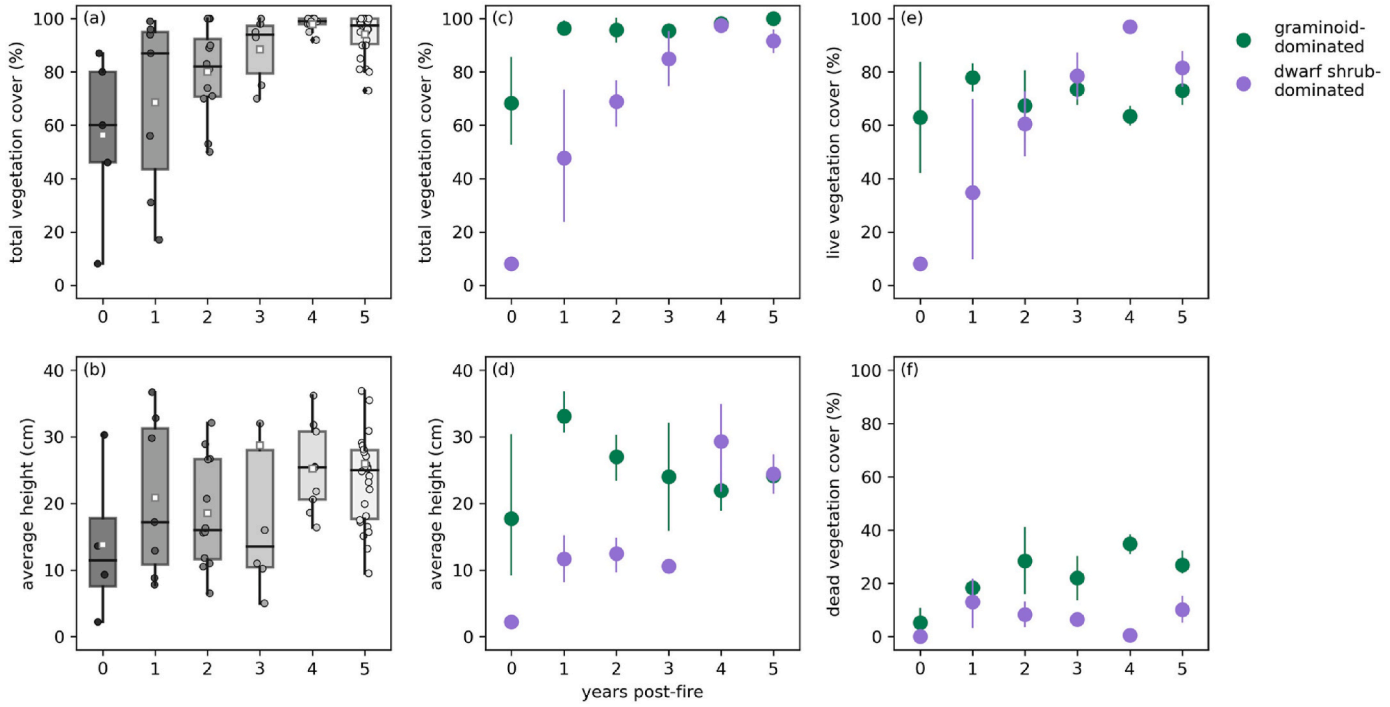

Fig. 11. Vegetation cover fractions and heights in wildfire areas across the South Pennines in different years post-fire (0 corresponds to wildfire areas from 2023, 5 to areas from 2018). a) and b) show data from all burned areas, c) to f) show means and standard deviations of the data categorised by dominant functional group.

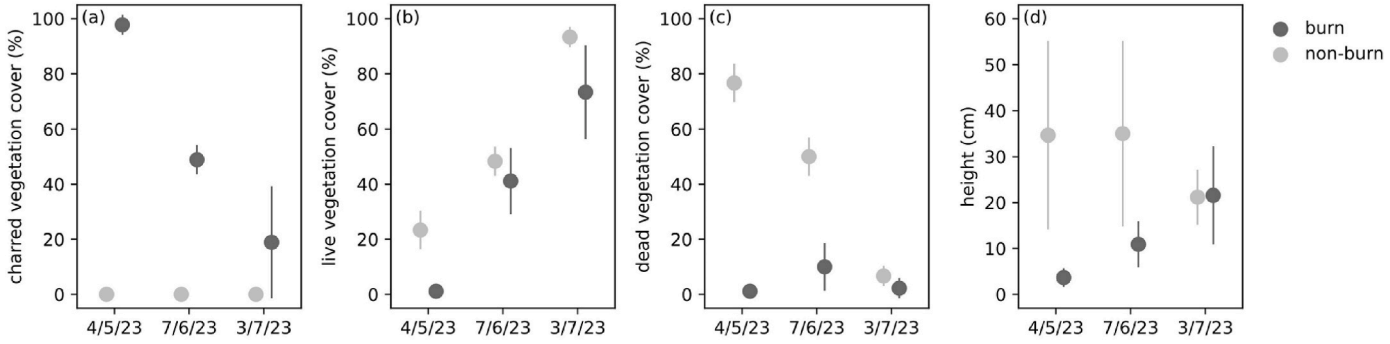

Fig. 12. Average vegetation cover fractions (a–c) and heights (d) inside (burn) and outside (non-burn) the Standedge wildfire area (burned on 03/05/23). The last measurement of vegetation height in the non-burn plots differed from the previous ones, either because of management (e.g. grazing), different measurement teams, or the effect of rain causing the grass to bend. Measurements from the same date were carried out consistently. Vertical lines represent the standard deviation.

Table 4
Coefficients in the selected regression model to explain spectral recovery times (reference category is acid grassland).

	Coefficient	Std. err.	p-value
Intercept	−292	84	0.001
Land cover – Bog	463	85	0.000
Land cover – Heather	418	72	0.000
Land cover – Heather grassland	276	94	0.005
Season – Summer	−213	101	0.038
Burn severity	1101	247	0.000
Snow cover days	11	4	0.004

Table 5
Coefficients in the regression model with interactions between variables.

	Coefficient	Std. err.	p-value
Intercept	17	74	0.815
Acid grassland: Burn severity: Spring	−169	315	0.594
Bog: Burn severity: Spring	1405	344	0.000
Heather: Burn severity: Spring	1489	266	0.000
Heather grassland: Burn severity: Spring	1036	412	0.015
Acid grassland: Burn severity: Summer	297	208	0.157
Bog: Burn severity: Summer	1362	248	0.000
Heather: Burn severity: Summer	727	209	0.001
Heather grassland: Burn severity: Summer	452	428	0.294
Snow cover days	12	4	0.000

Met Office Fire Severity Index (MOFSI) (Met Office, 2005). However, it is important to note that wildfires are not limited to the period estimated by the VIs. Particularly in acid grassland, the flammability window calculated from VIs covers a short period, as the optical signal changes rapidly with the onset of spring green-up. Cole et al. (2014) also found that PSRI declined particularly sharply in graminoid species compared to dwarf shrubs after reaching the annual maximum in April. However, the senescent biomass accumulated during winter persists as a flammable layer beneath the green grass shoots that dominate the spectral signal. This potentially contributes to the lower percentage of fires captured by the flammability window in acid grassland.

The longer flammability window observed for heather and heather grassland can be explained by the long winter dormancy of *Calluna,* which can last until late May or early June (Kwolek and Woolhouse, 1982). This period of dormancy is associated with low FMC and strong root resistance to water uptake (Bannister, 1964). FMC measurements in *Calluna* by Al-Moustafa et al. (2012) showed that FMC was still below 70% in May but increased to more than 100% in July. The longest flammability window was calculated for bog areas, despite their typically wet or waterlogged nature. However, the bogs in the South Pennines have historically experienced severe degradation, with lowered water tables transforming many sites into dry heath on peat (PDNPA, 2021). This could explain the similar phenological pattern of bog and heather, with bog sites showing even lower FMC levels in spring and summer, highlighting their vulnerability to severe wildfire events. While spring wildfires have predominantly impacted areas with a high proportion of senescent plant material, identifying flammable conditions in summer using VIs has been more challenging. This may be due to the fact that wildfire danger in summer primarily results from high temperatures and atmospheric drought, which leads to plant water loss but does not cause immediate mortality (Anderegg et al., 2013). Water stress can be observed to some extent in the NDMI, and other indices such as the MSI could be included, but meteorological indices may be better suited to identify critical periods over the summer. In general, our results are consistent with recent observations by Nikonovas et al. (2024) showing that fire regimes in UK upland land cover types are strongly dependent on fuel phenology, with highest fire activity occurring during the dormant and early green-up period in spring, while extreme fire weather conditions can override the phenological fire barrier provided by green vegetation in summer.

4.2. Wildfire impact on VIs

Larger differences between pre- and post-fire SAVI, PSRI, and NDMI observations during the summer months indicate a higher burn severity associated with summer fires. However, these disparities could also be influenced by the higher pre-fire values of SAVI and NDMI in summer compared to spring. Removal and charring of plants generally result in a reduction of these VIs through a decrease in reflectance in the NIR range and unchanged or even increased reflectance in the SWIR range, as the absorption of the latter by leaf water is reduced (Fassnacht et al., 2021). The largest change was found in NDMI, and other studies also reported that the largest wildfire-induced decrease was in wetness indices such as NDMI and NBR (Serra-Burriel et al., 2021). Differences in PSRI, which is sensitive to the carotenoid/chlorophyll ratio (Sims and Gamon, 2002), showed subtle changes and reflected distinct behaviours between spring and summer. In spring, the abundant senescent plant material is lost from the site and partly transformed into charcoal (Clay and Worrall, 2011), leading to a reduction in carotenoid reflectance. In contrast, during summer, the carotenoid to chlorophyll ratio is typically low, and the combustion of green plants therefore affects chlorophyll pigments more than carotenoids.

4.3. Spectral recovery of VIs and drivers of recovery

4.3.1. Acid grassland

VIs demonstrated high consistency in the rapid spectral recovery of acid grasslands, often within a year or even just two or three months. The main challenge in capturing this rapid recovery with remotely sensed VIs was data gaps in the satellite time series interrupting the short-lived signal. NDVI recovery was faster than SAVI for most grassland areas (by 32 days on average), indicating a lack of sensitivity of the index to different cover conditions as previously reported (Gao et al., 2000). The VI-estimated recovery times align well with the field observations of vegetation recovery at the Standedge wildfire area, where live vegetation cover was restored within a few weeks post-fire. Grass shoots also rapidly reached heights comparable to the surrounding unburned area, suggesting temporarily improved nutrient availability in the burned area (San Emeterio et al., 2016). Consequently, the land may be returned to pasture fairly quickly, and improvements in forage quality have also been reported for some species (Gimingham, 1972). Since the rate of fuel load accumulation is high in grass-dominated land cover classes, fuel availability for new wildfires is only temporarily reduced, although field data indicate that the proportion of dead biomass takes longer to reach pre-fire levels (around two years post-fire). However, accurately quantifying dead biomass fraction using satellite data is challenging due to the top view of the vegetation canopy. A study in subalpine grassland, where post-fire regeneration was generally slower than in our study, predicted that the return of the litter component could take several years (Wahren et al., 2001). Acid grassland wildfires exhibited a wide range of spectral changes in the VIs, but burn severity did not significantly impact their recovery times. The data indicate that acid grasslands recover faster spectrally after spring than summer fires, likely because areas burned in spring still have the entire growing season ahead. Following summer fires, plant growth is limited until the end of the growing season, which is why full spectral recovery can only be achieved in the following year (Fig. 10).

4.3.2. Heather

For heather land cover, estimated spectral recovery times varied significantly among wildfire areas, ranging from less than six months to approximately three years. The NBR recovery time was generally the longest, surpassing SAVI by approximately 90 days. This suggests that SWIR-based indices may be more effective at capturing heather recovery due to their higher sensitivity to vegetation structure. Conversely, the PSRI recovery times were the shortest, indicating that the noisy signal of the index is unsuitable for capturing the (assumed long-term) return of dead material within the heather canopy. Our model showed a significant effect of burn severity on recovery times in heather land cover, which has been reported in previous studies (Lees et al., 2021). This is typically attributed to the level of fuel consumption and ground heating affecting the regenerative capacity of *Calluna* (Gilbert, 2008; Grau-Andrés et al., 2019). Interestingly, recovery time increased more with burn severity in spring compared to summer. One possible explanation is that seed germination and plant development are delayed after severe spring fires because seeds are more likely to be exposed to drought conditions. Experiments by Birkeli et al. (2023) revealed that reduced water availability increases the time to germination and reduces the germination percentage of *Calluna* seeds, and also affects development in the seedling stage. Furthermore, post-fire development has been shown to depend on pre-fire stand age, with the ability to regenerate vegetatively strongly diminished in older stands, resulting in slower recovery (Davies et al., 2010b; Kayll and Gimingham, 1965). Since we lacked information on the age of the *Calluna* stands in our study area, we were unable to include this in the model. However, during our field campaign, we recorded the growth phase of *Calluna* on the wildfire scars and in the surrounding unburned areas, and found a similar pattern (Fig. S2a in supplementary material). When the unburned *Calluna* was in the mature-degenerate or degenerate phase, regeneration on the burned area primarily consisted of plants still in the pioneer phase, even on the oldest wildfire areas (from 2018). In contrast, stands burned in an earlier growth phase reached the building phase more rapidly (Fig. S2b in supplementary material). This aligns with the observations of Schellenberg and Bergmeier (2022), who noted that younger *Calluna* stands burned in the mature stage resprout vigorously and grow rapidly, allowing them to reach an early-mature stage after only three to four years under favourable conditions.

Generally, the VI-estimated recovery times for heather land cover underestimate the actual recovery time. Our field data suggest that cover in dwarf shrub-dominated areas is reconstituted faster than height, the latter taking four to five years and longer. Underestimates of recovery times may be due to the limited recovery time series available for some of the more recently burned areas. Additionally, VI-estimated

recovery times of less than one year for heather land cover may indicate either a misclassification in the LCM2021 or that the immediate post-fire signal is strongly dominated by other plant species, such as graminoids, herbs, and mosses. The LCM2021, as well as field observations of some rapidly recovering wildfire areas, suggest that these areas predominantly featured small *Calluna* patches before the fire, surrounded by graminoid-dominated acid grassland or bog vegetation (Fig. 13a). Where *Calluna* regeneration depends on seedling establishment, the rapid spread of pioneer species immediately after wildfire may hinder the germination of the light-sensitive *Calluna* seeds, possibly leading to a reduction in *Calluna* cover, as observed in other studies (Brys et al., 2005; Velle and Vandvik, 2014). However, if seedlings have established successfully, *Calluna* may regain dominance at a later stage of succession due to its superior competitiveness for light (Sedláková and Chytrỳ, 1999). Areas where *Calluna* is restricted to smaller patches and the potential for grass invasion from surrounding areas is high (potentially heather grasslands) could therefore be a target for post-wildfire management.

Our model also indicates that prolonged winter snow cover delays the recovery of burned areas. This could be attributed to lower seedling survival in winter when cold temperatures freeze the ground, leading to desiccation and browning of foliage (Legg et al., 1992), although a thick snow layer should prevent this. Extended periods of snow cover have also been known to be followed by plant damage caused by molds in early spring (Watson et al., 1966). They could also simply indicate sites with less favourable microclimates, such as those found at higher altitudes (Fig. 13b) or on north-facing slopes. In these areas, lower temperatures, high winds, or less sunlight limit plant growth, as suggested by this and other studies (Lees et al., 2021; Nilsen et al., 2005; Velle and Vandvik, 2014). Remaining unexplained variance in the recovery time may be attributed to differences in post-fire substrate conditions (Davies et al., 2010b).

4.3.3. Heather grassland and bog

We do not provide a separate discussion for heather grasslands, as they can be considered to hold an intermediary status between the previously discussed land cover classes from a remote sensing perspective. We hypothesise that the strong influence of grasses on the spectral signal likely contributes to relatively short estimated recovery times.

For bog, recovery estimates were similarly variable as for heather, ranging from a few months to up to five years. Our field campaign revealed that bog areas encompassed both pure graminoid and *Calluna*-dominated habitats, as the land cover class is defined by a soil characteristic (>0.5 m peat), which explains the large variability in recovery times. The discrepancy between NDVI and SAVI recovery suggests that soil background has a strong influence in bog areas, as darker soils in particular lead to higher NDVI values for incomplete canopies (Gao et al., 2000). We therefore recommend using SAVI instead. The NDMI exhibited the longest recovery time among all VIs, suggesting that wildfires can have a substantial impact on the moisture regime in moorlands. Wildfires alter the structure and water-holding capacity of peat soils depending on environmental factors such as landscape morphology, fire intensity, and resulting char composition: pyrolysed peat often exhibits increased hydrophobicity, which reduces water infiltration and increases surface runoff (Wu et al., 2020), diminishing soil water retention and affecting water availability for regenerating vegetation. c

4.4. Limitations and outlook

Our study based on the land cover classification of the LCM2021. However, we noted that the vegetation composition within one land cover class was highly variable in some areas. Therefore, we recommend that future studies map relative fractions of dwarf shrubs and graminoids to better distinguish areas dominated by different functional types. These could also be used to assess changes between pre- and post-fire vegetation composition. We also lacked information on management in the study area, which may have led to unquantifiable variability in the data and uncertainties in estimated recovery times. While our field measurements provided valuable insights into post-fire recovery based on a space-for-time sampling, future work should include long-term monitoring of wildfire areas, particularly in areas of slow recovery, to directly validate satellite-based estimates.

We focused our analyses solely on optical remote sensing data, as we aimed to investigate these data comprehensively. While they provide insight into important fuel properties, they offer limited information on the physical structure of the vegetation and therefore cannot fully capture vegetation recovery to pre-fire levels. In addition, the time series feature large gaps due to frequent cloud cover in the study area, which we overcame by using harmonic modelling to estimate baseline recovery, but which complicated the accurate estimation of recovery times. Therefore, future studies should include complementary information from sensors that are independent of atmospheric conditions and more sensitive to vegetation structure, such as SAR. The backscatter signal from spaceborne SAR has already been successfully used to retrieve information on *Calluna* height (Schmidt et al., 2018) and to monitor post-fire vegetation recovery in Arctic tundra (Zhou et al., 2019). Previous work on using the SAR intensity and InSAR coherence signal to detect burn scars in peat moorlands in the PDNP could be developed further to understand vegetation recovery in these landscapes (Millin-Chalabi et al., 2013). Canopy height and *Calluna* growth phase can also be determined from photogrammetric point clouds derived from high-resolution UAV imagery (Mead and Arthur, 2020; Neumann et al., 2020). Access to this information would facilitate more accurate assessments of when biomass (i.e., fuel load) is fully restored in burned areas. However, estimating the litter component remains difficult even with other sensors. Our study centered on the spectral recovery of remote sensing signals and the recovery of vegetation cover and height

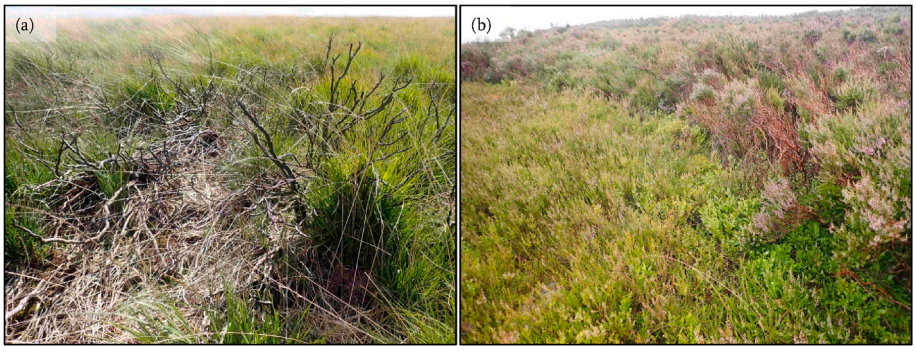

Fig. 13. a) Graminoid invasion of burned heather patch. b) Slow recovery on a higher altitude site burned in 2018, showing the transition between burned (left) and unburned (right) area.

in the field, with particular emphasis on fuel availability and condition. This should not be mistaken for the ecological recovery of an area, which requires more complex criteria such as assessments of biodiversity, structural diversity, and ecosystem functionality.

5. Conclusion

This study demonstrated the utility of optical VIs such as SAVI, NDMI, and PSRI for characterising the phenology of important fuel properties in UK upland land cover classes and identifying periods of peak vegetation flammability. Analysis of pre- and post-fire signals allowed a better understanding of wildfire-induced changes in the VIs and their recovery patterns in different land cover classes. Bog and heather exhibited the longest spectral recovery times, heather grassland was intermediate, and acid grassland recovered most rapidly. Our results underscore the importance of distinguishing between different functional groups when estimating vegetation recovery from remote sensing data across large areas, particularly between dwarf shrubs and graminoids. In addition to land cover class, recovery times were affected by burn severity, season, and winter snow cover. The comparison with field data from wildfire areas showed that optical data tend to underestimate the time required for recovery to pre-fire conditions, especially for habitats dominated by slower-growing dwarf shrubs. Future studies could supplement the optical data with SAR imagery or point cloud data, which provide additional information on vegetation structure, to improve recovery estimates. Our results advance the knowledge of phenology-driven fuel dynamics in moorlands and help to interpret satellite-based analysis of vegetation recovery. They serve as an important foundation for the development of satellite-based monitoring of fire risk and post-fire vegetation recovery, which can ultimately inform both precautionary measures and land management priorities.

CRediT authorship contribution statement

Pia Labenski: Writing – original draft, Visualization, Methodology, Formal analysis, Data curation, Conceptualization. **Gail Millin-Chalabi:** Writing – review & editing, Data curation, Conceptualization. **Ana María Pacheco-Pascagaza:** Writing – review & editing, Data curation, Conceptualization. **Johannes Antenor Senn:** Writing – review & editing, Data curation. **Fabian Ewald Fassnacht:** Writing – review & editing, Supervision, Funding acquisition, Conceptualization. **Gareth D. Clay:** Writing – review & editing, Supervision, Funding acquisition, Conceptualization.

Declaration of competing interest

The authors declare that they have no known competing financial interests or personal relationships that could have appeared to influence the work reported in this paper.

Data availability

Data will be made available on request.

Acknowledgements

PL and JAS received funding from the German Federal Ministry of Food and Agriculture as part of the project 'ErWiN' (2219WK54A4). AMPP, GM-C, and GDC were supported by funding from the Natural Environment Research Council (NE/T003553/1). We thank the following site owners and managers for permission to access the field areas: Moors for the Future Partnership, National Trust Marsden Moor, Royal Society for the Protection of Birds (RSPB) Dovestone, United Utilities, Enville and Stalybridge Estates, Staffordshire Wildlife Trust. A huge thanks goes to Martina Ettlin for her invaluable fieldwork assistance.

Appendix A. Supplementary data

Supplementary data to this article can be found online at https://doi.org/10.1016/j.indic.2024.100492.

References

Al-Moustafa, T., Armitage, R.P., Danson, F.M., 2012. Mapping fuel moisture content in upland vegetation using airborne hyperspectral imagery. Rem. Sens. Environ. 127, 74–83. https://doi.org/10.1016/j.rse.2012.08.034.

Albertson, K., Aylen, J., Cavan, G., McMorrow, J., 2009. Forecasting the outbreak of moorland wildfires in the English Peak District. J. Environ. Manag. 90, 2642–2651. https://doi.org/10.1016/j.jenvman.2009.02.011.

Albertson, K., Aylen, J., Cavan, G., McMorrow, J., 2010. Climate change and the future occurrence of moorland wildfires in the Peak District of the UK. Clim. Res. 45, 105–118. https://doi.org/10.3354/cr00926.

Anderegg, L.D., Anderegg, W.R., Berry, J.A., 2013. Not all droughts are created equal: translating meteorological drought into woody plant mortality. Tree Physiol. 33, 701–712. https://doi.org/10.1093/treephys/tpt044.

Armitage, R.P., Alberto Ramirez, F., Mark Danson, F., Ogunbadewa, E.Y., 2013. Probability of cloud-free observation conditions across Great Britain estimated using MODIS cloud mask. Remote Sensing Letters 4, 427–435. https://doi.org/10.1080/2150704X.2012.744486.

Arnell, N.W., Freeman, A., Gazzard, R., 2021. The effect of climate change on indicators of fire danger in the UK. Environ. Res. Lett. 16, 044027. https://doi.org/10.1088/1748-9326/abd9f2.

Badi, A.H.A., 2019. Remote Sensing to Characterise Vegetation Fuel Moisture Content in the UK Uplands (PhD Thesis). University of Salford (United Kingdom).

Bannister, P., 1964. The water relations of certain heath plants with reference to their ecological amplitude: II. Field studies. J. Ecol. 52, 481–497. https://doi.org/10.2307/2257845.

Billett, M.F., Charman, D.J., Clark, J.M., Evans, C.D., Evans, M.G., Ostle, N.J., Worrall, F., Burden, A., Dinsmore, K.J., Jones, T., McNamara, N.P., Parry, L., Rowson, J.G., Rose, R., 2010. Carbon balance of UK peatlands: current state of knowledge and future research challenges. Clim. Res. 45, 13–29. https://doi.org/10.3354/cr00903.

Birkeli, K., Gya, R., Haugum, S.V., Velle, L.G., Vandvik, V., 2023. Germination and seedling growth of Calluna vulgaris is sensitive to regional climate, heathland succession, and drought. Ecol. Evol. 13, e10199. https://doi.org/10.1002/ece3.10199.

Boelman, N.T., Rocha, A.V., Shaver, G.R., 2011. Understanding burn severity sensing in Arctic tundra: exploring vegetation indices, suboptimal assessment timing and the impact of increasing pixel size. Int. J. Rem. Sens. 32, 7033–7056. https://doi.org/10.1080/01431161.2011.611187.

Brys, R., Jacquemyn, H., De Blust, G., 2005. Fire increases aboveground biomass, seed production and recruitment success of Molinia caerulea in dry heathland. Acta Oecol. 28, 299–305. https://doi.org/10.1016/j.actao.2005.05.008.

Burgan, R.E., 1979. Estimating live fuel moisture for the 1978 national fire danger rating system. Intermountain Forest and Range Experiment Station, Forest Service. U.S. Department of Agriculture.

Chávez, R.O., Estay, S.A., Lastra, J.A., Riquelme, C.G., Olea, M., Aguayo, J., Decuyper, M., 2023. Npphen: an R-package for detecting and mapping extreme vegetation anomalies based on remotely sensed phenological variability. Rem. Sens. 15, 73. https://doi.org/10.3390/rs15010073.

Clay, G.D., Worrall, F., 2011. Charcoal production in a UK moorland wildfire – how important is it? J. Environ. Manag. 92, 676–682. https://doi.org/10.1016/j.jenvman.2010.10.006.

Coffelt, J.L., Livingston, R.K., 2002. Second U.S. Geological Survey Wildland Fire Workshop: Los Alamos, New Mexico, October 31-November 3, 2000. U.S. Geological Survey. https://doi.org/10.3133/ofr0211.

Cole, B., McMorrow, J., Evans, M., 2014. Spectral monitoring of moorland plant phenology to identify a temporal window for hyperspectral remote sensing of peatland. ISPRS J. Photogrammetry Remote Sens. 90, 49–58. https://doi.org/10.1016/j.isprsjprs.2014.01.010.

Costa, H., de Rigo, D., ibertà, G., Durrant, T.H., San-Miguel-Ayanz, J., 2020. European Wildfire Danger and Vulnerability under a Changing Climate. Publications Office of the European Union. https://doi.org/10.2760/46951.

Davies, G.M., 2005. Fire Behaviour and Impact on Heather Moorland (PhD Thesis). University of Edinburgh, Edinburgh.

Davies, G.M., Legg, C.J., Smith, A.A., MacDonald, A.J., 2009. Rate of spread of fires in Calluna vulgaris-dominated moorlands. J. Appl. Ecol. 46, 1054–1063. https://doi.org/10.1111/j.1365-2664.2009.01681.x.

Davies, G.M., Legg, C.J., O'hara, R., MacDonald, A.J., Smith, A.A., 2010a. Winter desiccation and rapid changes in the live fuel moisture content of Calluna vulgaris. Plant Ecol. Divers. 3, 289–299. https://doi.org/10.1080/17550874.2010.544335.

Davies, G.M., Smith, A.A., MacDonald, A.J., Bakker, J.D., Legg, C.J., 2010b. Fire intensity, fire severity and ecosystem response in heathlands: factors affecting the regeneration of Calluna vulgaris. J. Appl. Ecol. 47, 356–365. https://doi.org/10.1111/j.1365-2664.2010.01774.x.

Fassnacht, F.E., Schmidt-Riese, E., Kattenborn, T., Hernández, J., 2021. Explaining Sentinel 2-based dNBR and RdNBR variability with reference data from the bird's eye (UAS) perspective. Int. J. Appl. Earth Obs. Geoinf. 95, 102262. https://doi.org/10.1016/j.jag.2020.102262.

Forestry Commission, 2023. Wildfire statistics for England: report to 2020-21. Forestry Commission. https://www.gov.uk/government/publications/forestry-commission-wildfire-statistics-for-england-report-to-2020-21.
Galbraith, C.A., Stroud, D.A., 2022. Sites of Special Scientific Interest (SSSIs) in England: Their Historical Development and Prospects in a Changing Environment (No. NECR414). Natural England.
Gao, B., 1996. NDWI—a normalized difference water index for remote sensing of vegetation liquid water from space. Rem. Sens. Environ. 58, 257–266. https://doi.org/10.1016/S0034-4257(96)00067-3.
Gao, X., Huete, A.R., Ni, W., Miura, T., 2000. Optical–biophysical relationships of vegetation spectra without background contamination. Rem. Sens. Environ. 74, 609–620. https://doi.org/10.1016/S0034-4257(00)00150-4.
Gilbert, J.A., 2008. Calluna Vulgaris Regeneration on Upland Moorland Post-wildfire. University of Central Lancashire (PhD Thesis).
Gimingham, C.H., 1972. Ecology of Heathlands. Chapman and Hall.
Graham, A.M., Pope, R.J., Pringle, K.P., Arnold, S., Chipperfield, M.P., Conibear, L.A., Butt, E.W., Kiely, L., Knote, C., McQuaid, J.B., 2020. Impact on air quality and health due to the Saddleworth Moor fire in northern England. Environ. Res. Lett. 15, 074018. https://doi.org/10.1088/1748-9326/ab8496.
Grau-Andrés, R., Davies, G.M., Waldron, S., Scott, E.M., Gray, A., 2019. Increased fire severity alters initial vegetation regeneration across Calluna-dominated ecosystems. J. Environ. Manag. 231, 1004–1011. https://doi.org/10.1016/j.jenvman.2018.10.113.
Guerini Filho, M., Kuplich, T.M., Quadros, F.L.F.D., 2020. Estimating natural grassland biomass by vegetation indices using Sentinel 2 remote sensing data. Int. J. Rem. Sens. 41, 2861–2876. https://doi.org/10.1080/01431161.2019.1697004.
Hancock, M.H., 2008. An exceptional Calluna vulgaris winter die-back event, Abernethy Forest, Scottish Highlands. Plant Ecol. Divers. 1, 89–103. https://doi.org/10.1080/17550870802260772.
Harper, A., 2020. Vegetation Fires in Temperate Upland Heaths: Environmental Impacts, Recovery, and Management Implications (PhD Thesis). Swansea University.
Met Office, Hollis, D., McCarthy, M., Kendon, M., Legg, T., 2023. HadUK-grid gridded climate observations on a 1km grid over the UK, v1.2.0.ceda (1836-2022). NERC EDS Centre for Environmental Data Analysis. https://doi.org/10.5285/46f8c1377f8849eeb8570b8ac9b26d86. https://dx.doi.org/10.5285/46f8c1377f8849eeb8570b8ac9b26d86.
Huete, A.R., 1988. A soil-adjusted vegetation index (SAVI). Rem. Sens. Environ. 25, 295–309. https://doi.org/10.1016/0034-4257(88)90106-X.
Kayll, A.J., Gimingham, C.H., 1965. Vegetative regeneration of Calluna vulgaris after fire. J. Ecol. 729–734. https://doi.org/10.2307/2257631.
Keane, R.E., 2015. Wildland Fuel Fundamentals and Applications. Springer International Publishing, Cham. https://doi.org/10.1007/978-3-319-09015-3.
Kennedy, R.E., Yang, Z., Cohen, W.B., 2010. Detecting trends in forest disturbance and recovery using yearly Landsat time series: 1. LandTrendr — temporal segmentation algorithms. Rem. Sens. Environ. 114, 2897–2910. https://doi.org/10.1016/j.rse.2010.07.008.
Kirkpatrick, H., 2013. Chapter 16: managing moorland in the UK. In: Diemont, W.H., Heijman, W.J.M., Siepel, H., Webb, N.R. (Eds.), Economy and Ecology of Heathlands: Heathland Ecology and Management. KNNV Publishing, Zeist, The Netherlands.
Kruse, F.A., Lefkoff, A.B., Boardman, Y.J., Heidebrecht, K.B., Shapiro, A.T., Barloon, P.J., Goetz, A.F.H., 1993. The spectral image processing system (SIPS)—interactive visualization and analysis of imaging spectrometer data. Remot. Sens. Environ. 44 (2–3), 145–163.
Kwolek, A.V.A., Woolhouse, H.W., 1982. Studies on the dormancy of Calluna vulgaris (L.) Hull, during winter: the effect of photoperiod and temperature on the induction of dormancy and the annual cycle of development. Ann. Bot. 49, 367–376. https://doi.org/10.1093/oxfordjournals.aob.a086261.
Lees, K.J., Buxton, J., Boulton, C.A., Abrams, J.F., Lenton, T.M., 2021. Using satellite data to assess management frequency and rate of regeneration on heather moorlands in England as a resilience indicator. Environmental Research Communications 3, 085003. https://doi.org/10.1088/2515-7620/ac1a5f.
Legg, C.J., Maltby, E., Proctor, M.C.F., 1992. The ecology of severe moorland fire on the North York Moors: seed distribution and seedling establishment of Calluna vulgaris. J. Ecol. 737–752. https://doi.org/10.2307/2260863.
Lewis, C.H.M., Little, K., Graham, L.J., Kettridge, N., Ivison, K., 2024. Diurnal fuel moisture content variations of live and dead Calluna vegetation in a temperate peatland. Sci. Rep. 14, 4815. https://doi.org/10.1038/s41598-024-55322-z.
Liu, W., Guan, H., Hesp, P.A., Batelaan, O., 2023. Remote sensing delineation of wildfire spatial extents and post-fire recovery along a semi-arid climate gradient. Ecol. Inf. 78, 102304. https://doi.org/10.1016/j.ecoinf.2023.102304.
Lutes, D.C., Keane, R.E., Caratti, J.F., Key, C.H., Benson, N.C., Sutherland, S., Gangi, L.J., 2006. FIREMON: Fire Effects Monitoring and Inventory System (No. RMRS-GTR-164. Gen. Tech. Rep. U.S. Department of Agriculture, Forest Service, Rocky Mountain Research Station, Fort Collins, CO.
Mac Arthur, A., Malthus, T., 2012. Calluna vulgaris foliar pigments and spectral reflectance modelling. Int. J. Rem. Sens. 33, 5214–5239. https://doi.org/10.1080/01431161.2012.659357.
Maltby, E., Legg, C.J., Proctor, M.C.F., 1990. The ecology of severe moorland fire on the North York Moors: effects of the 1976 fires, and subsequent surface and vegetation development. J. Ecol. 490–518. https://doi.org/10.2307/2261126.
Marston, C., Rowland, C.S., O'Neil, A.W., Morton, R.D., 2022. Land cover map 2021 (10m classified pixels, GB). https://doi.org/10.5285/a22baa7c-5809-4a02-87e0-3cf87d4e223a.
McMorrow, J., 2011. Wildfire in the United Kingdom: status and key issues. In: Proc. 2nd Conf. On the Human Dimensions of Wildland Fire, pp. 44–56.
Mead, L., Arthur, M., 2020. Environmental condition in British moorlands: quantifying the life cycle of Calluna vulgaris using UAV aerial imagery. Int. J. Rem. Sens. 41, 573–583. https://doi.org/10.1080/2150704X.2019.1646931.
Merzlyak, M.N., Gitelson, A.A., Chivkunova, O.B., Rakitin, V.Y.U., 1999. Non-destructive optical detection of pigment changes during leaf senescence and fruit ripening. Physiol. Plantarum 106, 135–141. https://doi.org/10.1034/j.1399-3054.1999.106119.x.
Met Office, 2005. UK fire severity index [[WWW Document]. URL. https://www.metoffice.gov.uk/public/weather/fire-severity-index/#?tab=map&fcTime=1695981600&zoom=5&lon=-4.00&lat=55.74, 9.29.23.
Metzger, C.M.H., Heinichen, J., Eickenscheidt, T., Drösler, M., 2017. Impact of land-use intensity on the relationships between vegetation indices, photosynthesis and biomass of intensively and extensively managed grassland fens. Grass and Forage. Science 72, 50–63. https://doi.org/10.1111/gfs.12223.
Millin-Chalabi, G., 2016. Radar Multi-Temporal and Multi-Sensor Approach to Characterise Peat Moorland Burn Scars and Assess Burn Scar Persistence in the Landscape (PhD Thesis). The University of Manchester, United Kingdom.
Millin-Chalabi, G., McMorrow, J., Agnew, C., 2013. Detecting a moorland wildfire scar in the Peak District, UK, using synthetic aperture radar from ERS-2 and Envisat ASAR. Int. J. Rem. Sens. 35, 54–69. https://doi.org/10.1080/01431161.2013.860658.
Moors for the Future, 2023. Wildfire recording system [WWW Document]. URL. https://www.wildfirelog.co.uk/, 6.15.23.
Neumann, C., Behling, R., Schindhelm, A., Itzerott, S., Weiss, G., Wichmann, M., Müller, J., 2020. The colors of heath flowering – quantifying spatial patterns of phenology in Calluna life-cycle phases using high-resolution drone imagery. Remote Sens Ecol Conserv 6, 35–51. https://doi.org/10.1002/rse2.121.
Newville, M., Stensitzki, T., Allen, D.B., Ingargiola, A., 2014. LMFIT: non-linear least-square minimization and curve-fitting for Python. https://doi.org/10.5281/zenodo.11813.
Nichol, C.J., Grace, J., 2010. Determination of leaf pigment content in Calluna vulgaris shoots from spectral reflectance. Int. J. Rem. Sens. 31, 5409–5422. https://doi.org/10.1080/01431160903302957.
Nikonovas, T., Santín, C., Belcher, C.M., Clay, G.D., Kettridge, N., Smith, T.E.L., Doerr, S.H., 2024. Vegetation phenology as a key driver for fire occurrence in the UK and comparable humid temperate regions. Int. J. Wildland Fire 33. https://doi.org/10.1071/WF23205.
Nilsen, L.S., Johansen, L., Velle, L.G., 2005. Early stages of Calluna vulgaris regeneration after burning of coastal heath in central Norway. Appl. Veg. Sci. 8, 57–64. https://doi.org/10.1111/j.1654-109X.2005.tb00629.x.
Ordnance Survey, 2023. OS Terrain 5 [WWW document]. Ordnance Survey. URL. https://www.ordnancesurvey.co.uk/products/os-terrain-5, 10.13.23.
Pasquarella, V.J., Arévalo, P., Bratley, K.H., Bullock, E.L., Gorelick, N., Yang, Z., Kennedy, R.E., 2022. Demystifying LandTrendr and CCDC temporal segmentation. Int. J. Appl. Earth Obs. Geoinf. 110, 102806. https://doi.org/10.1016/j.jag.2022.102806.
PDNPA, 2013. Landscape: peak District state of the Park report [WWW Document]. URL. http://www.peakdistrict.gov.uk/microsites/sopr/landscape, 6.21.23.
PDNPA, 2021. Climate change vulnerability assessment by the peak District national Park authority [WWW Document]. URL. https://reports.peakdistrict.gov.uk/ccva/, 9.28.23.
Pearson, R.K., Neuvo, Y., Astola, J., Gabbouj, M., 2016. Generalized Hampel filters. EURASIP Journal on Advances in Signal Processing 2016 87. https://doi.org/10.1186/s13634-016-0383-6.
Perry, M.C., Vanvyve, E., Betts, R.A., Palin, E.J., 2022. Past and future trends in fire weather for the UK. Nat. Hazards Earth Syst. Sci. 22, 559–575. https://doi.org/10.5194/nhess-22-559-2022.
Pickell, P.D., Hermosilla, T., Frazier, R.J., Coops, N.C., Wulder, M.A., 2016. Forest recovery trends derived from Landsat time series for North American boreal forests. Int. J. Rem. Sens. 37, 138–149. https://doi.org/10.1080/2150704X.2015.1126375.
Potter, C., 2018. Recovery rates of wetland vegetation greenness in severely burned ecosystems of Alaska derived from satellite image analysis. Rem. Sens. 10, 1456. https://doi.org/10.3390/rs10091456.
Prichard, S.J., Rowell, E., Keane, R.E., Hudak, A.T., Lutes, D., Loudermilk, E.L., 2023. Wildland fuel characterization across space and time. In: Landscape Fire, Smoke, and Health. American Geophysical Union (AGU), pp. 53–68. https://doi.org/10.1002/9781119757030.ch4.
Rein, G., Huang, X., 2021. Smouldering wildfires in peatlands, forests and the arctic: challenges and perspectives. Current Opinion in Environmental Science & Health 24, 100296. https://doi.org/10.1016/j.coesh.2021.100296.
Rouse, J.W., Haas, R.H., Schell, J.A., Deering, D.W., 1974. Monitoring vegetation systems in the great plains with ERTS. In: NASA. Goddard Space Flight Center, 3d ERTS-1 Symp.
San Emeterio, L., Múgica, L., Ugarte, M.D., Goicoa, T., Canals, R.M., 2016. Sustainability of traditional pastoral fires in highlands under global change: effects on soil function and nutrient cycling. Agric. Ecosyst. Environ. 235, 155–163. https://doi.org/10.1016/j.agee.2016.10.009.
San-Miguel-Ayanz, J., Schulte, E., Schmuck, G., Camia, A., Strobl, P., Libertà, G., Giovando, C., Boca, R., Sedano, F., Kempeneers, P., McInerney, D., Withmore, C., Oliveira, S., Rodrigues, M., Durrant, T., Corti, P., Oehler, F., Vilar, L., Amatulli, G., 2012. Comprehensive monitoring of wildfires in europe: the European forest fire information system (EFFIS). In: Approaches to Managing Disaster - Assessing Hazards, Emergencies and Disaster Impacts. https://doi.org/10.5772/28441.
Sankey, J.B., Wallace, C.S.A., Ravi, S., 2013. Phenology-based, remote sensing of post-burn disturbance windows in rangelands. Ecol. Indicat. 30, 35–44. https://doi.org/10.1016/j.ecolind.2013.02.004.

Schellenberg, J., Bergmeier, E., 2022. The Calluna life cycle concept revisited: implications for heathland management. Biodivers. Conserv. 31, 119–141. https://doi.org/10.1007/s10531-021-02325-1.

Schepers, L., Haest, B., Veraverbeke, S., Spanhove, T., Vanden Borre, J., Goossens, R., 2014. Burned area detection and burn severity assessment of a heathland fire in Belgium using airborne imaging spectroscopy (APEX). Rem. Sens. 6, 1803–1826. https://doi.org/10.3390/rs6031803.

Schmidt, J., Fassnacht, F.E., Förster, M., Schmidtlein, S., 2018. Synergetic use of Sentinel-1 and Sentinel-2 for assessments of heathland conservation status. Remote Sensing in Ecology and Conservation 4, 225–239. https://doi.org/10.1002/rse2.68.

Sedláková, I., Chytrý, M., 1999. Regeneration patterns in a Central European dry heathland: effects of burning, sod-cutting and cutting. Plant Ecol. 143, 77–87. https://doi.org/10.1023/A:1009807411654.

Serra-Burriel, F., Delicado, P., Prata, A.T., Cucchietti, F.M., 2021. Estimating heterogeneous wildfire effects using synthetic controls and satellite remote sensing. Rem. Sens. Environ. 265, 112649. https://doi.org/10.1016/j.rse.2021.112649.

Shepherd, M.J., Labadz, J., Caporn, S.J., Crowle, A., Goodison, R., Rebane, M., Waters, R., 2013. Natural England Review of Upland Evidence - Restoration of Degraded Blanket Bog (No. NEER003), Natural England Evidence Review. Natural England.

Sims, D.A., Gamon, J.A., 2002. Relationships between leaf pigment content and spectral reflectance across a wide range of species, leaf structures and developmental stages. Rem. Sens. Environ. 81, 337–354. https://doi.org/10.1016/S0034-4257(02)00010-X.

Taylor, A., Bruce, M., Britton, A., Owen, J., Gagkas, Z., Pohle, I., Fielding, D., Hadden, R., 2022. Fire Danger Rating System (FDRS) Report (Technical Report). James Hutton Institute, Aberdeen, Scotland.

Thomaz, S.M., Agostinho, A.A., Gomes, L.C., Silveira, M.J., Rejmánek, M., Aslan, C.E., Chow, E., 2012. Using space-for-time substitution and time sequence approaches in invasion ecology. Freshw. Biol. 57, 2401–2410. https://doi.org/10.1111/fwb.12005.

Van der Wal, R., Bonn, A., Monteith, D., Reed, M., Blackstock, K., Hanley, N., Thompson, D., Evans, M., Alonso, Isabel, 2011. Chapter 5: mountains, moorlands and heaths. In: The UK National Ecosystem Assessment Technical Report. UK National Ecosystem Assessment. UNEP-WCMC, Cambridge, pp. 105–160.

Velle, L.G., Vandvik, V., 2014. Succession after prescribed burning in coastal C alluna heathlands along a 340-km latitudinal gradient. J. Veg. Sci. 25, 546–558. https://doi.org/10.1111/jvs.12100.

Verbesselt, J., Hyndman, R., Newnham, G., Culvenor, D., 2010. Detecting trend and seasonal changes in satellite image time series. Rem. Sens. Environ. 114, 106–115.

Villarreal, M.L., Norman, L.M., Buckley, S., Wallace, C.S.A., Coe, M.A., 2016. Multi-index time series monitoring of drought and fire effects on desert grasslands. Rem. Sens. Environ. 183, 186–197. https://doi.org/10.1016/j.rse.2016.05.026.

Wahren, C.-H., Papst, W.A., Williams, R.J., 2001. Early post-fire regeneration in subalpine heathland and grassland in the Victorian Alpine National Park, south-eastern Australia. Austral Ecol. 26, 670–679. https://doi.org/10.1046/j.1442-9993.2001.01151.x.

Wang, Z., Ma, Y., Zhang, Y., Shang, J., 2022. Review of remote sensing applications in grassland monitoring. Rem. Sens. 14, 2903. https://doi.org/10.3390/rs14122903.

Watson, A., Miller, G., Green, F.H.W., 1966. Winter browning of Heather (Calluna vulgaris) and other moorland plants. Trans. Bot. Soc. Edinb. 40, 195–203. https://doi.org/10.1080/03746606608685143.

Wilson, E.H., Sader, S.A., 2002. Detection of forest harvest type using multiple dates of Landsat TM imagery. Rem. Sens. Environ. 80, 385–396. https://doi.org/10.1016/S0034-4257(01)00318-2.

Wu, Y., Zhang, N., Slater, G., Waddington, J.M., de Lannoy, C.-F., 2020. Hydrophobicity of peat soils: characterization of organic compound changes associated with heat-induced water repellency. Sci. Total Environ. 714, 136444. https://doi.org/10.1016/j.scitotenv.2019.136444.

Xu, J., Morris, P.J., Liu, J., Holden, J., 2018. Hotspots of peatland-derived potable water use identified by global analysis. Nat. Sustain. 1, 246–253. https://doi.org/10.1038/s41893-018-0064-6.

Yallop, A.R., Thacker, J.I., Thomas, G., Stephens, M., Clutterbuck, B., Brewer, T., Sannier, C.a.D., 2006. The extent and intensity of management burning in the English uplands. J. Appl. Ecol. 43, 1138–1148. https://doi.org/10.1111/j.1365-2664.2006.01222.x.

Zhou, Z., Liu, L., Jiang, L., Feng, W., Samsonov, S.V., 2019. Using long-term SAR backscatter data to monitor post-fire vegetation recovery in tundra environment. Rem. Sens. 11, 2230. https://doi.org/10.3390/rs11192230.

Zhu, Z., Woodcock, C.E., 2014. Continuous change detection and classification of land cover using all available Landsat data. Rem. Sens. Environ. 144, 152–171. https://doi.org/10.1016/j.rse.2014.01.011.